Isotopic Composition and Accurate Mass

3

Learning Objectives

- Isotopic composition of elements and their effect on mass spectra
- Translation of isotopic abundances into mass spectral patterns
- Analytical information from isotopic patterns
- Nominal and accurate mass of molecules and ions
- Mass resolution and its effects on isotopic patterns and mass accuracy
- Accurate mass as a tool for determining molecular formulas
- Ultrahigh resolution – aspects and applications
- Relevance of these topics for all types of mass spectral analyses

In the context of general chemistry we rarely pay attention to the different isotopes of the individual elements involved in a reaction. For instance, the molecular mass of tribromomethane, $CHBr_3$, is usually calculated as 252.73 g mol^{-1} on the basis of relative atomic mass from the Periodic Table. In mass spectrometry, however, we need to more accurately consider individual isotopes, because mass spectrometry is based upon the separation of ions by mass-to-charge ratio, *m*/*z* [1–3]. Thus, there actually is no molecular ion peak at *m*/*z* 252.73 in the mass spectrum of tribromomethane. Instead, major peaks occur at *m*/*z* 250, 252, 254, and 256 accompanied by some minor other ones.

In order to successfully interpret a mass spectrum, one needs to understand isotopic masses and their relation to the atomic weights, isotopic abundances, and the resulting isotopic patterns, and finally, high-resolution and accurate mass measurements. These issues are closely related to each other, offer a wealth of analytical information, and are valid for any type of mass spectrometer and any ionization method employed. Therefore, the content of this chapter is of highest relevance for the interpretation of any kind of mass spectral data.

J.H. Gross, *Mass Spectrometry*, DOI 10.1007/978-3-319-54398-7_3

3.1 Isotopic Classification of the Elements

An element is specified by the number of protons in its nucleus. This equals the *atomic number Z* of the respective element and determines its place within the periodic table of the elements. The atomic number is given as a subscript preceding the elemental symbol, e.g., $_6$C in case of carbon. Atoms with nuclei of the same atomic number differing in the number of neutrons are termed *isotopes*. One isotope differs from another isotope of the same element in that it possesses a different *number of neutrons N*, i.e., by the *mass number A* or *nucleon number*. The mass number of an isotope is given as a superscript preceding the elemental symbol, e.g., ^{12}C. The mass number *A* is the sum of the total number of protons and neutrons in an atom, molecule, or ion [4].

$$A = Z + N \tag{3.1}$$

Mass and order
The *mass number* must not be confused with the *atomic number* of an element. For the heavier atoms there can be isotopes of the same mass number belonging to different elements, e.g., the most abundant isotopes of both $_{18}$Ar and $_{20}$Ca have mass number 40.

3.1.1 Monoisotopic Elements

Among 83 naturally occurring stable elements, 20 elements do exist in the form of only one single naturally occurring stable isotope. Therefore, they are termed *monoisotopic elements*, i.e., all of their atoms have equal *A*. Among the monoisotopic elements, fluorine (^{19}F), sodium (^{23}Na), phosphorus (^{31}P), and iodine (^{127}I) belong to the more prominent examples in organic mass spectrometry. Nonetheless, there are many more such as beryllium (^{9}Be), aluminum (^{27}Al), manganese (^{55}Mn), cobalt (^{59}Co), arsenic (^{75}As), niobium (^{93}Nb), rhodium (^{103}Rh), cesium (^{133}Cs), and gold (^{197}Au). The monoisotopic elements are also referred to as A or X elements [5, 6]. If radioactive isotopes were also taken into account, not a single monoisotopic element would remain.

3.1.2 Di-isotopic Elements

Several elements exist naturally in two isotopes and within the context of mass spectrometry it is useful to deal with them as a class of their own. Nevertheless, the term *di-isotopic element* is not an official one, i.e., not part of IUPAC nomenclature. These elements can even be sub-classified into those having one isotope that is 1 u heavier than the most abundant isotope and those having one isotope that is 2 u heavier than the most abundant isotope. The first group has been termed A + 1 or

X + 1 elements, the latter ones have been termed A + 2 or X + 2 elements, respectively [5, 6]. If we do not restrict our view to the elements typically encountered in organic mass spectrometry, one should add the class of X–1 elements with one minor isotope of 1 u lower mass than the most abundant one.

Prominent examples of X + 1 elements are hydrogen (^{1}H, $^{2}H \equiv D$), carbon (^{12}C, ^{13}C), and nitrogen (^{14}N, ^{15}N). Deuterium (D) is of low abundance (0.0115%) and therefore, hydrogen is usually treated as a monoisotopic or as an X element, which is a valid approximation, even if a hundred hydrogens are contained in a molecule.

Among the X + 2 elements, chlorine (^{35}Cl, ^{37}Cl) and bromine (^{79}Br, ^{81}Br) are relatively common, but copper (^{63}Cu, ^{65}Cu), gallium (^{69}Ga, ^{71}Ga), silver (^{107}Ag, ^{109}Ag), indium (^{113}In, ^{115}In), and antimony (^{121}Sb, ^{123}Sb) also belong to this group. Even though occurring in more than two isotopes, some other elements such as oxygen, sulfur, and silicon, can be dealt with as X + 2 elements for practical reasons. As long as only a few oxygens are part of a formula, oxygen might even be treated as an X element because of the low abundances of ^{17}O and ^{18}O.

Finally, the elements lithium (^{6}Li, ^{7}Li), boron (^{10}B, ^{11}B), and vanadium (^{50}V, ^{51}V) come along with a lighter isotope of lower abundance than the heavier one and thus, they can be grouped together as X–1 elements.

Atomic numbers, mass numbers, and isotopes Let us apply the notation of Eq. (3.1) to the elements contributing to a molecule of tribromomethane that has already been mentioned in the introductory paragraph of this chapter. The molecule is composed of carbon, hydrogen, and bromine, the latter occurs naturally as two isotopes of almost equal abundance. Thus, these four species are most relevant for the $CHBr_3$ molecule (Fig. 3.1). Now we get an idea of why tribromomethane molecular ions appear split into several peaks in a mass spectrum. We will return to this topic shortly.

3.1.3 Polyisotopic Elements

The majority of elements are grouped as *polyisotopic elements* because they consist of three or more isotopes showing a wide variety of isotopic distributions.

3.1.4 Representation of Isotopic Abundances

Isotopic abundances are listed either as their sum being 100% or with the abundance of the most abundant isotope normalized to 100%. The first normalization is

Fig. 3.1 Atomic numbers and mass numbers relevant for the elements contributing to tribromomethane, $CHBr_3$

obvious as it reflects all isotopes as contributing to 100% of an element. The second normalization (also used throughout this book) is commonly applied in mass spectrometry: mass spectra are customarily reported as normalized to the base peak or at least to the most intensive peak within the *m*/*z* range of interest (Chap. 1). The isotopic classifications and *isotopic compositions* of some common elements are listed below (Table 3.1).

Check mode of normalization
Care has to be taken when comparing isotopic abundances from different sources as they might be compiled using one *or* the other procedure of normalization. Never mix normalization modes in your calculations!

Bar graph representations are much better suited for visualization of isotopic compositions than tables, and in fact they exactly show how such a distribution would appear in a mass spectrum (Fig. 3.2). This appearance coined the term *isotopic pattern* or *isotope pattern*.

Note
Some authors use the term *isotopic cluster*, which is incorrect, as *cluster* refers to an associate of more atoms, molecules, or ions of the same species, sometimes associated with one other species, e.g., $[Ar_n]^{+\bullet}$, $[(H_2O)_nH]^+$, and $[I(CsI)_n]^-$ are cluster ions.

3.1.5 Calculation of Atomic, Molecular, and Ionic Mass

3.1.5.1 Nominal Mass

In order to calculate the approximate mass of a molecule we usually sum up integer masses of the elements encountered, e.g., for CO_2 we calculate the mass as 12 u + 2 × 16 u = 44 u. The result of this simple procedure is not particularly precise but provides acceptable values for simple molecules. This is called *nominal mass* [6].

More precisely, the nominal mass of an element is defined as the *integer mass* of its most abundant naturally occurring stable isotope [6]. The nominal mass of an element is often equal to the integer mass of the lowest mass isotope of that element, e.g., for H, C, N, O, S, Si, P, F, Cl, Br, I (Table 3.1). The nominal mass of an ion is the sum of the nominal masses of its constituent elements.

Nominal mass of trifluoroacetic acid The nominal mass of trifluoroacetic acid, CF_3COOH, is calculated based on the mass number of the most abundant isotopes of the contributing elements. Using ^1H, ^{12}C, ^{16}O, and ^{19}F we obtain 1 u + 2 × 12 u + 2 × 16 u + 3 × 19 u = 114 u.

Table 3.1 Isotopic classifications and isotopic compositions of some common elements

Classification	Atomic symbol	Atomic number Z	Mass number A	Isotopic composition	Isotopic mass [u]	Relative atomic mass [u]
(X)[a]	H	1	1	100	1.007825	1.00795
			2	0.0115	2.014101	
X	F	9	19	100	18.998403	18.998403
X	Na	11	23	100	22.989769	22.989769
X	P	15	31	100	30.973762	30.973762
X	I	53	127	100	126.904468	126.904468
X + 1	C	6	12	100	12.000000[b]	12.0108
			13	1.08	13.003355	
X + 1	N	7	14	100	14.003074	14.00675
			15	0.369	15.000109	
(X + 2)[a]	O	8	16	100	15.994915	15.9994
			17	0.038	16.999132	
			18	0.205	17.999161	
(X + 2)[a]	Si	14	28	100	27.976927	28.0855
			29	5.0778	28.976495	
			30	3.3473	29.973770	
(X + 2)[a]	S	16	32	100	31.972071	32.067
			33	0.80	32.971459	
			34	4.52	33.967867	
			36	0.02	35.967081	
X + 2	Cl	17	35	100	34.968853	35.4528
			37	31.96	36.965903	
X + 2	Br	35	79	100	78.918338	79.904
			81	97.28	80.916291	
X–1	Li	3	6	8.21	6.015122	6.941
			7	100	7.016004	
X–1	B	5	10	24.8	10.012937	10.812
			11	100	11.009306	
poly	Xe	54	124	0.33	123.905896	131.29
			126	0.33	125.904270	
			128	7.14	127.903530	
			129	98.33	128.904779	
			130	15.17	129.903508	
			131	78.77	130.905082	
			132	100	131.904154	
			134	38.82	133.905395	
			136	32.99	135.907221	

A complete table is provided in the Appendix. © IUPAC 2001 [7, 8]
[a]Classification in parentheses means "not in the strict sense"
[b]Standard of atomic mass scale

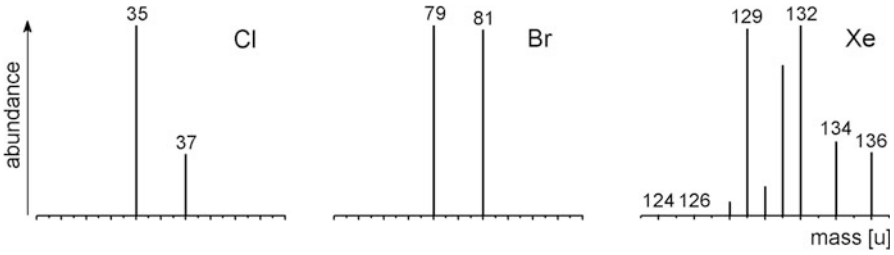

Fig. 3.2 Isotopic patterns of chlorine, bromine, and xenon. The bar graph representations of the isotopic distributions have the same optical appearance as mass spectra. You should compare these graphical representations to the compositions listed in Table 3.1. Afterwards, you may decide for yourself which type you would consider to be easier to perceive and to compare

Nominal mass of $SnCl_2$ To calculate the nominal mass of $SnCl_2$, the masses of ^{120}Sn and ^{35}Cl have to be used, i.e., 120 u + 2 × 35 u = 190 u. While the ^{35}Cl isotope represents the most abundant as well as the lowest mass isotope of chlorine, ^{120}Sn is the most abundant but not the lowest mass isotope of tin which is ^{112}Sn.

Mass versus mass number
When dealing with nominal mass, mass number and nominal mass both have the same numerical value. However, the *mass number* is dimensionless and must not be confused with *nominal mass* in units of u.

3.1.5.2 Isotopic Mass

The *isotopic mass* is the exact mass of an isotope. It is very close to but not equal to the nominal mass of the isotope (Table 3.1). The only exception is the carbon isotope ^{12}C which has an isotopic mass of 12.000000 u.

The *unified atomic mass* [u] is defined as $^1/_{12}$ of the mass of one atom of nuclide ^{12}C which has been assigned precisely 12 u, where 1 u = 1.660538 × 10^{-27} kg [4, 6, 9, 10]. This convention dates back to 1961 [2].

Avoid using outdated masses
The *unified atomic mass* [u], defined as $^1/_{12}$ of the mass of one atom of nuclide ^{12}C is the only valid unit for atomic mass. Mass values from dated literature can be ambiguous. Prior to 1961, physicists defined the *atomic mass unit* [amu] based on $^1/_{16}$ of the mass of one atom of nuclide ^{16}O. The definition of chemists was based on the relative atomic mass of oxygen which is somewhat higher due to the nuclides ^{17}O and ^{18}O that also occur in natural oxygen [2]. Thus, the oxygen-based mass scales are neither compatible among each other nor are the mass values equal to the actual ^{12}C–based scale. You *always* should be using u and *never* amu.

3.1.5.3 Relative Atomic Mass

The *relative atomic mass* or the *atomic weight* as it is also often imprecisely termed is calculated as the weighted average of the naturally occurring isotopes of an element [6]. The weighted average $M_{\mathrm{r.}}$ is calculated from

$$M_r = \frac{\sum_{i=1}^{i} A_i \times m_i}{\sum_{i=1}^{i} A_i} \tag{3.2}$$

with A_{i} being the abundances of the isotopes and m_{i} their respective isotopic masses [11]. For this purpose, the abundances can be used in any numerical form or normalization as long as they are used consistently.

Atomic mass of chlorine The relative atomic mass of chlorine is 35.4528 u. However, there is such atom. Instead, chlorine is composed of ^{35}Cl (34.968853 u) and ^{37}Cl (36.965903 u), the former making up 75.78% and the latter 24.22% – or having relative abundances of 100% and 31.96%, respectively (Table 3.1 and Fig. 3.2). According to Eq. (3.2), we would calculate the relative atomic mass of chlorine as $M_{\mathrm{r.}} = (100 \times 34.968853\ \mathrm{u} + 31.96 \times 36.965903\ \mathrm{u})/(100 + 31.96) = 35.4528\ \mathrm{u}$.

3.1.5.4 Monoisotopic Mass

The exact mass of the most abundant isotope of an element is termed *monoisotopic mass* [6]. The monoisotopic mass of a molecule is the sum of the monoisotopic masses of the elements in its empirical formula. As mentioned before, the monoisotopic mass is not necessarily the naturally occurring isotope of lowest mass. However, for the common elements in organic mass spectrometry the monoisotopic mass is obtained using the mass of the lowest mass isotope of that element, because this is also the most abundant isotope of the respective element (Sect. 3.1.5.1).

Monoisotopic mass of trifluoroacetic acid The monoisotopic mass of trifluoroacetic acid, CF_3COOH, is calculated based on the isotopic masses of the most abundant isotopes of the contributing elements. Using ^{1}H, ^{12}C, ^{16}O, and ^{19}F we obtain $1.007825\ \mathrm{u} + 2 \times 12.000000\ \mathrm{u} + 2 \times 15.994915\ \mathrm{u} + 3 \times 18.998403\ \mathrm{u} = 113.992864\ \mathrm{u}$. While the result is very close to the nominal mass 114 u, it still differs by 0.007136 u from that value.

3.1.5.5 Relative Molecular Mass

The *relative molecular mass*, M_{r}, or *molecular weight* is calculated from the relative atomic masses of the elements contributing to the empirical formula [6]. With the exception of very large molecules of say $>10^3$ u the relative molecular mass is rarely useful in mass spectrometry.

Molecular weight of tribromomethane Let's once more revisit tribromomethane. Using the relative atomic mass of H, C, and Br from Table 3.1 the molecular mass of $CHBr_3$ is calculated as 1.0079 u + 12.0108 u + 3 × 79.9040 u = 252.7307 u.

3.1.5.6 Exact Ionic Mass

The *exact mass of a positive ion* formed by the removal of one or more electrons from a molecule is equal to its monoisotopic mass minus the mass of the electron(s), m_e [4]. For negative ions, the electron mass (0.000548 u) has to be added accordingly.

Exact mass of a $CO_2^{+\bullet}$ ion The exact mass of the carbon dioxide molecular ion, $CO_2^{+\bullet}$, is calculated as 12.000000 u + 2 × 15.994915 u – 0.000548 u = 43.989282 u.

3.1.5.7 Role of the Electron Mass When Calculating Exact Mass

The question remains whether the mass of the electron m_e (5.48×10^{-4} u) has really to be taken into account. This issue was of almost pure academic interest as long as mass spectrometry was limited to mass accuracies of several 10^{-3} u. As FT-ICR, Orbitrap, and even recent oaTOF instruments deliver mass accuracies in the order of $<10^{-3}$ u, one should routinely include the electron mass in calculations [12, 13]. Here, neglecting the electron mass would cause a systematic error of the size of m_e, which is unacceptable when mass measurement accuracies in the order of $<10^{-3}$ u are to be achieved.

3.1.5.8 Number of Decimals When Calculating Exact Mass

The isotopic masses provided in this book are listed with six decimal places corresponding to an accuracy of 10^{-6} u (Table 3.1 and Appendix A.2), which is about three orders of magnitude below typical mass errors in mass spectrometry (± 0.001 u).

The number of decimal places one should employ in mass calculations depends on the purpose they are used for. In the *m/z* range of up to about 500 u, the use of isotopic mass with four decimal places may provide sufficient accuracy. Above that, at least five decimal places are required, because the increasing number of atoms results in an unacceptable multiplication of many small mass errors. The results of those calculations may again be reported with only four decimal places (± 0.0001 u), because this is sufficient for most applications.

Exact mass of mellitin $[M + H]^+$ ions Mellitin is the major active component of the honey bee venom. Mellitin is a peptide consisting of 26 amino acids with a molecular formula of $C_{131}H_{229}N_{39}O_{31}$. Let us calculate the exact mass of the protonated molecule, $[M + H]^+$, based on isotopic masses rounded to three and four decimals, respectively, and finally, based on full six decimals (Table 3.2). The resulting mass based on four decimals already deviates from the accurate result by 0.0051 u, the mass based on only three decimals is off by unacceptable 0.0405 u.

Table 3.2 Calculation of the exact mass of $[M + H]^+$ ions of the peptide mellitin based on different levels of accuracy

Element	Mass, three decimals [u]	Mass, four decimals [u]	Mass exact [u]	Number of atoms
C	12.000	12.0000	12.000000	131
H	1.008	1.0078	1.007825	230
N	14.003	14.0031	14.003074	39
O	15.995	15.9949	15.994915	31
Summed mass minus m_e	2845.802	2845.7563	2845.761453	

3.1.6 Natural Variations in Relative Atomic Mass

The masses of isotopes can be measured with accuracies better than *parts per billion* (ppb), e.g., $m_{40Ar} = 39.9623831235 \pm 0.000000005$ u. Unfortunately, determinations of abundance ratios are less accurate, causing errors of several *parts per million* (ppm) in relative atomic mass. The real limiting factor, however, comes from the variation of isotopic abundances from natural samples, e.g., in case of lead (Pb) which is the final product of radioactive decay of uranium, the atomic weight varies by 500 ppm depending on the Pb/U ratios in the lead ore [11]. Variations in natural isotopic distributions are also responsible for the varying number of decimal places stated with the relative atomic masses in Table 3.1.

For organic mass spectrometry the case of carbon is of highest relevance. Carbon is ubiquitous in metabolic processes and the most prominent example of variations in the $^{13}C/^{12}C$ isotopic ratio is presented by the different pathways of CO_2 fixation during photosynthesis, causing $^{13}C/^{12}C$ ratios of 0.01085–0.01115. Petroleum, coal, and natural gas yield very low $^{13}C/^{12}C$ ratios of 0.01068–0.01099 and carbonate minerals, on the other side, set the upper limit at about 0.01125 [11]. Even proteins of different origin (plants, fish, mammals) can be distinguished by their $^{13}C/^{12}C$ ratios [14, 15].

Isotope ratio mass spectrometry (IR-MS) makes use of these facts to determine the origin or the age of a sample (Chap. 15). For convenience, the minor changes in isotopic ratios are expressed using the *delta notation* stating the deviation of the isotopic ratio from a defined standard in parts per thousand (‰) [11, 16]. The delta value of carbon, $\delta^{13}C$, for example, is calculated from:

$$\delta^{13}C(‰) = \left[\left({}^{13}C/{}^{12}C_{sample}\right)/\left({}^{13}C/{}^{12}C_{standard}\right) - 1\right] \times 1000 \qquad (3.3)$$

The internationally accepted standard value for $^{13}C/^{12}C_{standard}$ is 0.0112372 as represented by belemnite from the Pee Dee formation, i.e., for PDP $\delta^{13}C = 0‰$ (PDB standard). PDB is a well-defined belemnite fossil from the Pee Dee formation of South Carolina, USA. For example, to calculate $\delta^{13}C$ by use of Eq. (3.3) for a

compound having $^{13}C/^{12}C_{sample} = 0.0109800$ we obtain $\delta^{13}C = [(0.0109800/0.0112372) - 1] \times 1000 = -22.88‰$.

Stable carbon isotope ratios of most natural materials of biological interest range from $\delta^{13}C = -100‰$ to about $\delta^{13}C = 0‰$ versus PDB (Fig. 3.3). These natural variations result from isotopic fractionation during physical, chemical, and biological processes. Inorganic carbon in seawater, freshwater, and carbonates has a rather high proportion of ^{13}C. Organic carbon, on the other side, is generally depleted of ^{13}C as a result of biological isotope fractionation, mostly due to kinetic isotope effects during photosynthesis [17]. Thus, the origin of food can be determined by employing $\delta^{13}C$ measurements, e.g., fruit/vegetables by country or whether the source of ethanol in alcoholic beverages is sugar cane, sugar beet, cereal starch, or obtained by synthetic processes [14, 16, 18].

Wool from western or eastern Ireland? Among numerous other applications, the $^{34}S/^{32}S$ isotope ratio has been exploited to determine whether wool originated from sheep living at or close to the west or east coast of Ireland [19]. The distance from the west coast at which Irish farm sheep were kept was found to be negatively correlated to the $\delta^{34}S$ values. The values changed from +15.8‰ for west coast wool to as low as +5.3‰ for east coast wool. In IR-MS, differences of >10‰ $\delta^{34}S$ are considered highly significant.

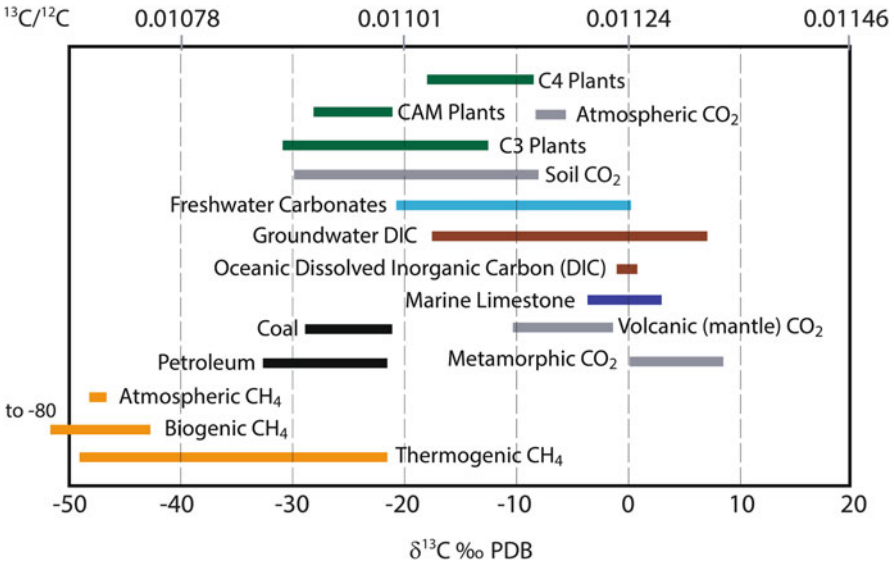

Fig. 3.3 Compilation of $\delta^{13}C$ values of different sources of carbon relative to PDB. The ratios of $^{13}C/^{12}C$ (rounded to five decimals) at $\delta^{13}C = -40‰, -20‰, 0‰, 20‰$ are shown for comparison to a more common scale (Adapted with kind permission from a figure by James Wittke, Northern Arizona University)

Common practice
Assuming an average ^{13}C content of 1.1%, equaling a $^{13}C/^{12}C$ ratio of 0.0111 has proven to be most useful in the majority of mass spectrometric applications.

3.2 Calculation of Isotopic Distributions

As long as we are dealing with molecular masses in a range of up to some 10^3 u, it is possible to separate ions which differ by 1 u in mass. The upper mass limit for their separation depends on the resolution of the instrument employed. Consequently, the isotopic composition of the analyte is directly reflected in the mass spectrum – it can be regarded as an elemental fingerprint.

Even if the analyte is chemically perfectly pure it represents a mixture of different isotopic compositions, provided it is not solely composed of monoisotopic elements. Therefore, a mass spectrum normally superimposes the mass spectra of all isotopic species involved [20]. The *isotopic distribution* or *isotopic pattern* of molecules containing one chlorine or bromine atom is listed in Table 3.1. But what about molecules containing two or more di-isotopic or even polyisotopic elements? While it may seem, at the first glance, to complicate the interpretation of mass spectra, isotopic patterns are in fact an ideal source of analytical information.

3.2.1 Carbon: An X + 1 Element

In the mass spectrum of methane (Fig. 1.6), there is a tiny peak at m/z 17 that has not been mentioned in the introduction. As one can infer from Table 3.1 this should result from the ^{13}C content of natural carbon which is an X + 1 element according to our classification.

How isotope patterns come about Imagine a total of 1000 methane molecules, CH_4. Due to a content of 1.1% ^{13}C, there will be 11 molecules containing ^{13}C instead of ^{12}C; the remaining 989 molecules are $^{12}CH_4$. Therefore, the ratio of relative intensities of the peaks at m/z 16 and m/z 17 is defined by the ratio 989/11 or by usual normalization 100/1.1.

In a more general way, carbon consists of ^{13}C and ^{12}C in a ratio r that can be written as $r = c/(100 - c)$ where c is the abundance of ^{13}C. Then, the probability to have only ^{12}C in a molecular ion M consisting of w carbons, i.e., the probability of monoisotopic ions P_M is given by [21]:

$$P_M = \left(\frac{100 - c}{100}\right)^w \tag{3.4}$$

The probability of having exactly one ^{13}C atom in an ion with w carbon atoms is therefore

$$P_{M+1} = w\left(\frac{c}{100 - c}\right)\left(\frac{100 - c}{100}\right)^w \tag{3.5}$$

and the ratio P_{M+1}/P_M is given as

$$\frac{P_{M+1}}{P_M} = w\left(\frac{c}{100 - c}\right) \tag{3.6}$$

In case of a carbon-only molecule such as the buckminster fullerene C_{60}, the ratio P_{M+1}/P_M becomes $60 \times 1.1/98.9 = 0.667$. If the monoisotopic peak at m/z 720 due to $^{12}C_{60}$ is regarded as 100%, the M + 1 peak due to $^{12}C_{59}{}^{13}C$ will have 66.7% relative intensity.

Estimate the intensity of the ^{13}C peak

For the $^{13}C/^{12}C$ ratio, the M + 1 peak intensity can be easily estimated in percent in a simplified manner, and with an insignificant error, by multiplying the number of carbon atoms by 1.1%, e.g., $60 \times 1.1\% = 66\%$.

There is again a certain probability for one of the remaining 59 carbon atoms to be ^{13}C rather than ^{12}C. After simplification of Beynon's approach [21] to be used for one atomic species only, the probability that there will be an ion containing two ^{13}C atoms is expressed by:

$$\frac{P_{M+2}}{P_M} = \frac{w}{2}\left(\frac{c}{100 - c}\right)(w - 1)\left(\frac{c}{100 - c}\right) = \frac{w(w - 1)c^2}{2(100 - c)^2} \tag{3.7}$$

For C_{60} the ratio P_{M+2}/P_M now becomes $(60 \times 59 \times 1.1^2)/(2 \times 98.9^2) = 0.219$, i.e., the M + 2 peak at m/z 722 due to $^{12}C_{58}{}^{13}C_2$ ions will show as 21.9% relative to the M peak, which definitely cannot be neglected. By extension of this principle, equations for the P_{M+3}/P_M ratio representing the third isotopic peak can be derived and so forth.

The calculation of isotopic patterns as just shown for the carbon-only molecule C_{60} can be done analogously for any X + 1 element. Furthermore, the application of this scheme is not restricted to molecular ions, but can also be used for fragment ions (Fig. 3.4). Nevertheless, care should be taken to assure that the presumed isotopic peak is not partially or even completely due to a different fragment ion, e.g., an ion containing one hydrogen more than the presumed X + 1 composition.

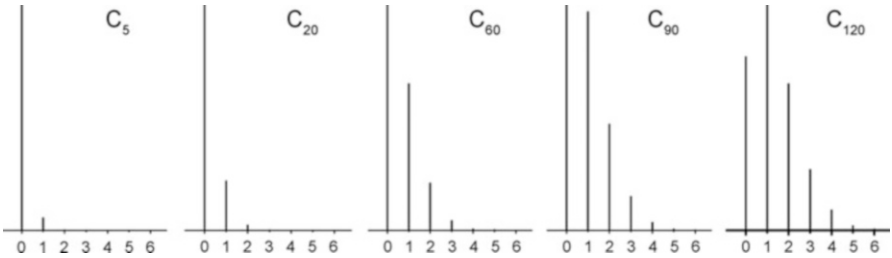

Fig. 3.4 Calculated isotopic patterns for carbon. Note the steadily expanding width of the pattern as X + 2, X + 3, X + 4,... become visible. At about C_{90} the X + 1 peak reaches the same intensity as the X peak. At higher carbon numbers it becomes the base peak of the pattern

Estimate the number of carbon atoms
It is very helpful to read out the P_{M+1}/P_M ratio from a mass spectrum to calculate the approximate number of carbon atoms. Provided no other element contributing to M + 1 is present, an M + 1 intensity of 15%, for example, indicates the presence of 14 carbons. (For possible overestimation due to autoprotonation cf. Sect. 7.2).

It is interesting how the width of the isotopic pattern increases as X + 2, X + 3, X + 4, ... become detectable. In principle, the isotopic pattern of C_w expands up to X + *w*, because even the composition $^{13}C_w$ is possible. As a result, the isotopic pattern of *w* atoms of a di-isotopic element consists at least theoretically of *w* + 1 peaks. However, the probability of extreme combinations is negligible and even somewhat more probable combinations are of no importance as long they are below about 0.1%. In practice, the interpretation of the carbon isotopic pattern is limited by experimental errors in relative intensities rather than by detection limits for peaks of low intensity. Such experimental errors can be due to poor signal-to-noise ratios (Sect. 1.6.3), autoprotonation (Sect. 7.2), or interference with other peaks.

At about C_{90} the X + 1 peak reaches the same intensity as the X peak, and at higher carbon number *w*, it becomes the base peak of the pattern, because the probability that an ion contains at least one ^{13}C becomes larger than that for the monoisotopic ion. A further increase in *w* makes the X + 2 signal stronger than the X and X + 1 peak and so on. A table with representative carbon isotopic abundances is provided in the Appendix.

3.2.2 Terms Related to Isotopic Composition

Molecules and ions of identical elemental composition but differing in isotopic composition are termed *isotopic homologs* or simply *isotopologs*. For example, $H_3C\text{-}CH_3$ and $H_3C\text{-}^{13}CH_3$ are isotopologs. Molecules and ions of identical isotopic

composition but differing in position of the isotopes are termed *isotopomers*. For example, $H_2C = CD_2$ and HDC = CHD are isotopomers.

The *isotopic molecular ion* (M + 1, M + 2, ...) is a molecular ion containing one or more of the less abundant naturally occurring isotopes of the atoms that make up the molecular structure [4]. This term can be generalized for any non-monoisotopic ion. Thus, *isotopic ions* are those ions containing one or more of the less abundant naturally occurring isotopes of the atoms that make up the ion.

The position of the most intensive peak of an isotopic pattern is termed *most abundant mass* [6], and the corresponding ion should be named *most abundant isotopolog* (*ion*). For example, the most abundant mass in case of C_{120} is 1441 u corresponding to M + 1 (Fig. 3.4). The most abundant mass is relevant in the case of large ions (Sect. 3.4.3).

3.2.3 Binomial Approach

The above stepwise treatment of X + 1, X + 2, and X + 3 peaks has the advantage that it can be followed easier, but it bears the disadvantage that an equation needs to be solved for each individual peak. Alternatively, one can calculate the relative abundances of the isotopic species for a di-isotopic element from a binomial expression [5, 22, 23]. In the term $(a + b)^n$ the isotopic abundances of both isotopes are given as a and b, respectively, and n is the number of this species in the molecule.

$$\begin{aligned}(a+b)^n = a^n + na^{n-1}b + n\,(n-1)\,a^{n-2}b^2/(2!)\\ +n\,(n-1)\,(n-2)\,a^{n-3}b^3/(3!) + \ldots\end{aligned} \tag{3.8}$$

For $n = 1$ the isotopic distribution can of course be directly obtained from the isotopic abundance table (Table 3.1 and Fig. 3.2) and in case of $n = 2$, 3, or 4 the expression can easily be solved by simple multiplication, e.g.,

$$\begin{aligned}(a+b)^2 &= a^2 + 2ab + b^2\\ (a+b)^3 &= a^3 + 3a^2b + 3ab^2 + b^3\\ (a+b)^4 &= a^4 + 4a^3b + 6a^2b^2 + 4ab^3 + b^4\end{aligned} \tag{3.9}$$

Again, we obtain $w + 1$ terms for the isotopic pattern of w atoms. The binomial approach works for any di-isotopic element, regardless of whether it is of X + 1, X + 2, or X–1 type. However, as the number of atoms increases, any manual calculation will grow more tedious and become more prone to error.

3.2.4 Halogens

The halogens Cl and Br occur in two isotopic forms, each of them being of significant abundance, whereas F and I are monoisotopic (Table 3.1). In most

cases there are only a few Cl and/or Br atoms in a molecule and this predestinates the binomial approach for this purpose.

Isotopic pattern by two chlorines The isotopic pattern of Cl_2 is calculated from Eq. (3.9) with the abundances $a = 100$ and $b = 31.96$ as $(100 + 31.96)^2 = 10{,}000 + 6392 + 1019$. After normalization we obtain 100 : 63.9 : 10.2 as the relative intensities of the three peaks. Any other normalization for the isotopic abundances would give the same result, e.g., $a = 0.7578$, $b = 0.2422$. The calculated isotopic pattern of Cl_2 can be understood from the following practical consideration: The two isotopes ^{35}Cl and ^{37}Cl can be combined in three different ways: (*i*) $^{35}Cl_2$ giving rise to the monoisotopic composition, (*ii*) $^{35}Cl^{37}Cl$ yielding the first isotopic peak which is here X + 2, and finally (*iii*) $^{37}Cl_2$ giving the second isotopic peak X + 4. Thus, two chlorines cause three peaks in total. The combinations with a higher number of chlorine atoms can be explained accordingly.

Expect *w* + 1 peaks
As already mentioned, the isotopic pattern of C_w expands up to X + *w*, because in theory even the composition $^{13}C_w$ is possible. In fact, for any di-isotopic element, the isotopic pattern of *w* atoms comprises *w* + 1 peaks, e.g., C_{10} yields 11 peaks, Cl_2 yields 3 peaks, and Br_4 yields 5 peaks (check by yourself in Figs. 3.4 and 3.5). Not all peaks may be clearly visible in the spectrum because the probability of some isotopic combinations can be negligible.

It is helpful to have frequent isotopic distributions at hand. For some Cl_x, Br_y, and Cl_xBr_y combinations these are tabulated in the Appendix. Tables are useful for the construction of isotopic patterns from "building blocks". Nevertheless, as visual information is easier to compare with a plotted spectrum, these patterns are also shown below (Fig. 3.5). In case of Cl and Br the peaks are always separated from each other by 2 u, i.e., the isotopic peaks are located at X + 2, 4, 6 and so on.

If there are two bromine or four chlorine atoms contained in the formula, the isotopic peaks become stronger than the monoisotopic peak, because the second isotope is of much higher abundance than in case of the ^{13}C isotope.

Quick estimate of Cl and Br patterns
Rapid estimation of the isotopic patterns of chlorine and bromine can be achieved with good results by using the approximate isotope ratios $^{35}Cl/^{37}Cl = 3 : 1$ and $^{79}Br/^{81}Br = 1 : 1$. Visual comparison with calculated patterns is also suitable (Fig. 3.5).

Decision-making help One may want to seek advice on how to distinguish between those patterns. For example, the patterns of Cl_2Br and Cl_3Br or of

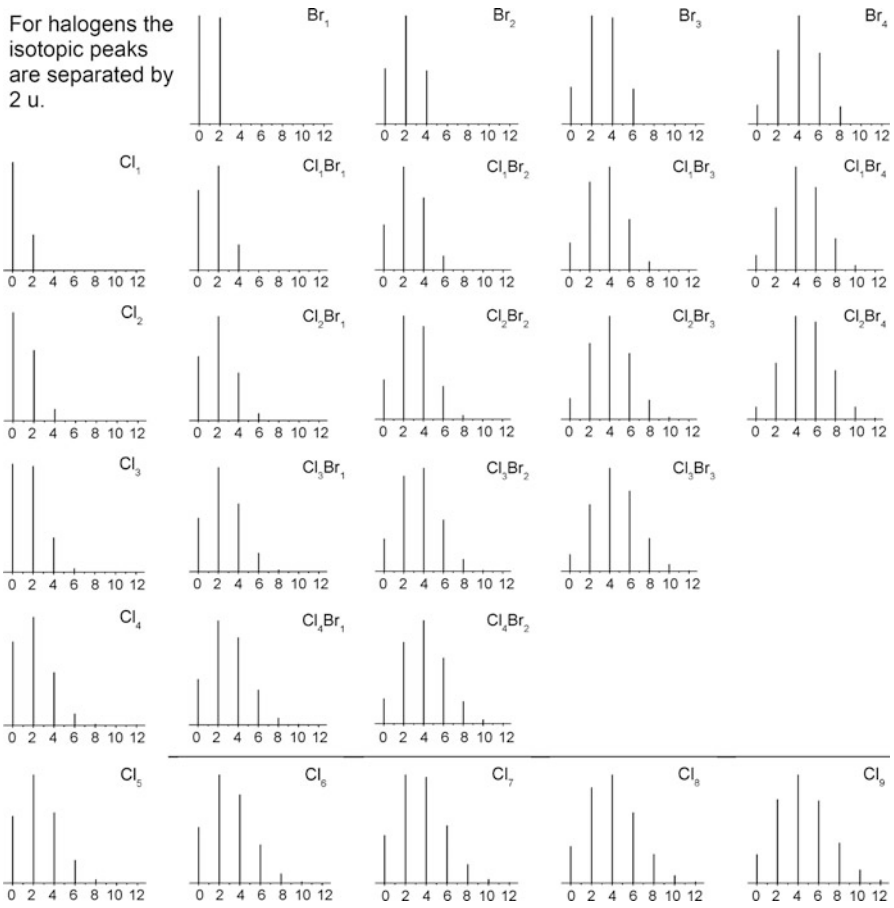

Fig. 3.5 Calculated isotopic patterns for combinations of bromine and chlorine. The peak shown at zero position corresponds to the monoisotopic ion at *m*/*z* X. The isotopic peaks are then located at *m*/*z* = X + 2, 4, 6, ... The numerical value of X is given by the mass number of the monoisotopic combination, e.g., 70 u for Cl_2

Cl_2Br_3 and Cl_3Br_3 closely resemble each other. To distinguish such pairs it is helpful to construct orientation lines between signal peak tips of comparable intensity. Generally these will decline with one pattern but can be positively inclined or even close to horizontal in others (Fig. 3.6).

Six bromine patterns united The EI mass spectrum of hexabromobenzene, C_6Br_6, is particularly illustrative in that it provides the complete series of isotope patterns from Br_1 to Br_6 in a row (Fig. 3.7). The series starts with the molecular ion, $[C_6Br_6]^{+\bullet}$, and proceeds via $[M–Br]^+$ and $[M–Br_2]^{+\bullet}$ down to the signals for $[C_6Br]^+$. This also shows that such patterns are not rare exceptions but have to be expected in real-world samples. For practicing purposes, you might want to compare the patterns in

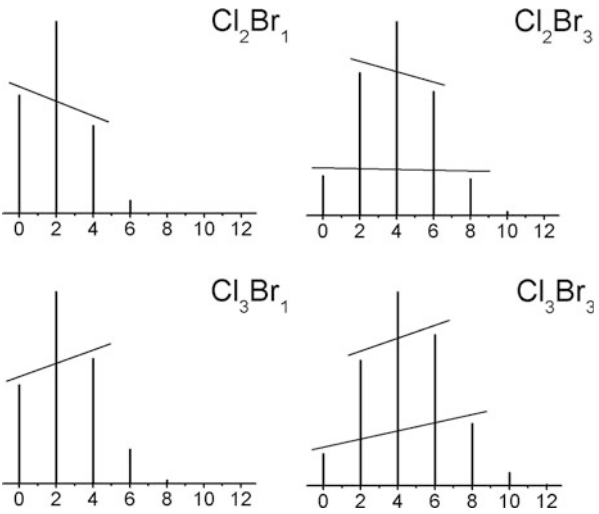

Fig. 3.6 Aid in distinguishing isotopic patterns by using orientation lines. *Left side:* patterns with four peaks each; *right side*: patterns with six peaks

the spectrum to those in Fig. 3.5. (For explanations on how these numerous ions come about refer to Chap. 6.)

3.2.5 Combinations of Carbon and Halogens

So far we have treated the X + 1 and the X + 2 elements separately, admittedly a rather artificial approach. The combination of C, H, N, and O with the halogens F, Cl, Br, and I covers a large fraction of the molecules one usually has to deal with. When regarding H, O, and N as X elements, which is a valid approximation for not too large molecules, the construction of isotopic patterns can be conveniently accomplished. By use of the isotopic abundance tables of the elements or of tables of frequent combinations of these as provided in this chapter or in the Appendix, the building blocks can be combined to obtain more complex isotopic patterns.

Construction of an isotopic pattern Let us construct the isotopic pattern of $C_9N_3Cl_3$ restricting ourselves to the isotopic contributions of C and Cl, i.e., with N as an X element. Here, the isotopic pattern of chlorine can be expected to be dominant over that of carbon. First, from the cubic form of Eq. (3.9) the Cl_3 pattern is calculated as follows: $(0.7578 + 0.2422)^3 = 0.435 + 0.417 + 0.133 + 0.014$ and after normalization this becomes 100 : 95.9 : 30.7 : 3.3. Of course, using the tabulated abundances of the Cl_3 distribution (Appendix) would be faster. The result is then plotted with 2 u distance, beginning at the nominal mass of the monoisotopic ion, i.e., 9×12 u + 3×14 u + 3×35 u = 255 u. The contribution of C_9 to the pattern is mainly at X + 1 where we have $9 \times 1.1\% = 9.9\%$, whereas its contribution to X + 2 (0.4%, Appendix) is negligible in this simple estimation. Finally, the

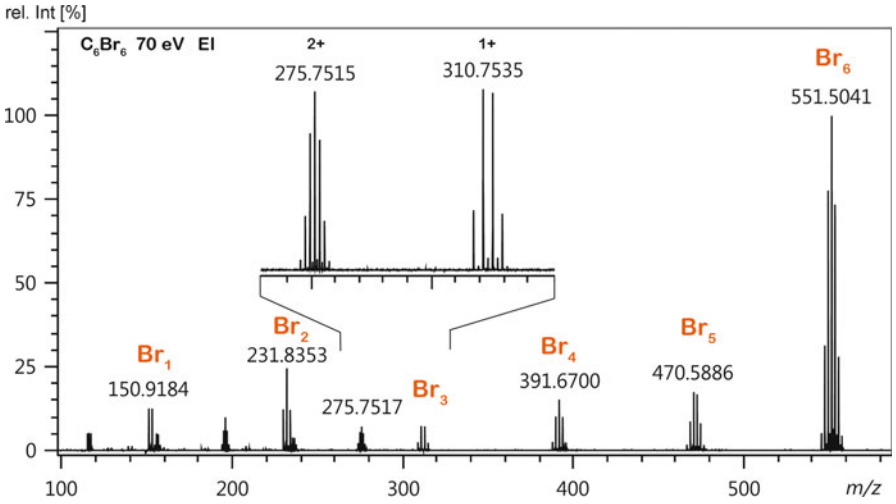

Fig. 3.7 70-eV EI mass spectrum of hexabromobenzene in the range *m/z* 100–580. The lower *m/z* range is omitted to allow for a clearer presentation of the bromine patterns. The number of bromines is annotated for convenience. The *m/z* labels provide accurate mass (Sect. 3.5) and refer to the most abundant signal of the respective isotope pattern. Watch how and where the pattern of the doubly charged molecular ion, M^{2+}, is displayed on the *m/z* scale next to the singly charged ion with a Br_3 pattern (*inset*)

X + 1 contribution of C_9 is placed into the gaps of the Cl_3 pattern each with 9.9% relative to the preceding peak of the chlorine isotopic distribution (Fig. 3.8).

3.2.6 Polynomial Approach

The polynomial approach is the logical expansion of the binomial approach. It is useful for the calculation of isotopic distributions of polyisotopic elements or for formulas composed of several non-monoisotopic elements [22, 23]. In general, the isotopic distribution of a molecule can be described by a product of polynominals

$$(a_1 + a_2 + a_3 + \ldots)^m \; (b_1 + b_2 + b_3 + \ldots)^n (c_1 + c_2 + c_3 + \ldots)^o + \ldots \qquad (3.10)$$

where a_1, a_2, a_3 etc. represent the individual isotopes of one element, b_1, b_2, b_3 etc. represent those of another and so on until all elements are included. The exponents m, n, o etc. give the number of atoms of these elements as contained in the empirical formula.

Calculating a complete pattern The complete isotopic distribution of stearic acid trichloromethylester, $C_{19}H_{35}O_2Cl_3$ is obtained according to Eq. (3.10) from polynomial expression

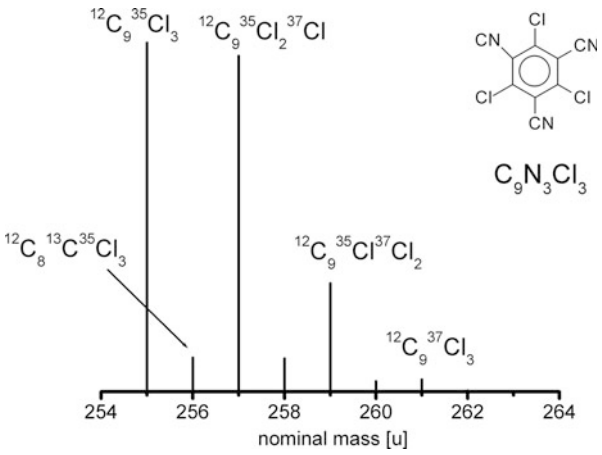

Fig. 3.8 The isotopic pattern of $C_9N_3Cl_3$ as constructed in the example above. The first ^{13}C isotopic peaks are located between the X + 2, 4, and 6 peaks of the dominant Cl_3 pattern. Nitrogen is treated as an X element and has been omitted from the peak labels for clarity

$$(A_{12C} + A_{13C})^{19} (A_{1H} + A_{2H})^{35} (A_{16O} + A_{17O} + A_{18O})^{2} (A_{35Cl} + A_{37Cl})^{3}$$

with A_x representing the relative abundances of the isotopes involved for each element. The problem with the calculation of isotopic patterns resides in the enormous number of terms obtained for larger molecules. Even for this simple example, the number of terms would be $(2)^{19} \times (2)^{35} \times (3)^2 \times (2)^3 = 1.297 \times 10^{18}$. The number is dramatically reduced if like terms are combined which describe the same isotopic composition regardless where the isotopes are located in the molecule. However, manual calculations are prone to become tedious if not impractical; computer programs now simplify the process [24, 25].

Software-based calculation of $C_{19}H_{35}O_2Cl_3$ isotope pattern Let us apply IsoPro 3.1, a freely available software program, to calculate the isotopic pattern of stearic acid trichloromethylester, $C_{19}H_{35}O_2Cl_3$. After entering the composition, it is just a matter of a mouse click to get the pattern either as a graphical display or as a mass list (Fig. 3.9). Obviously, the three chlorine atoms are dominating the appearance of the pattern and it is thus not surprising that the relative intensities are very similar to what we had in the case of $C_9N_3Cl_3$ (Fig. 3.8).

Knowing your software
Mass spectrometers usually are delivered with the software for calculating isotopic distributions. Similar programs are also offered as internet-based or shareware solutions [26, 27]. While such software is readily accessible, it is still necessary to obtain a thorough understanding of isotopic patterns as a prerequisite for adequately interpreting mass spectra.

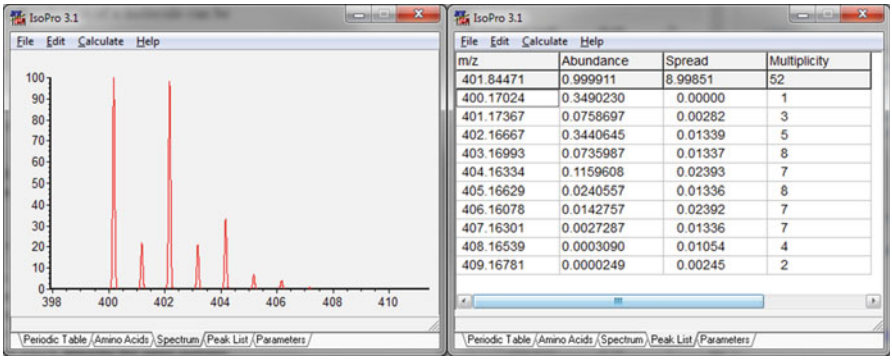

Fig. 3.9 Results from entering the formula $C_{19}H_{35}O_2Cl_3$ into IsoPro 3.1 isotopic distribution calculator [26]. The program provides either a customizable plot *(left)* or a peak list (*right*). Note that the list is normalized to 100% as equal to all species and that the *m/z* values provide accurate mass (Sect. 3.5)

3.2.7 Oxygen, Silicon, and Sulfur

Oxygen, silicon, and sulfur are polyisotopic elements in the strict sense – oxygen as ^{16}O, ^{17}O, and ^{18}O, sulfur as ^{32}S, ^{33}S, ^{34}S, and ^{36}S, and silicon as ^{28}Si, ^{29}Si, and ^{30}Si. The isotopic patterns of sulfur and silicon are by far not as prominent as those of chlorine and bromine, but still important.

^{17}O (0.038%) and ^{18}O (0.205%) are so rare that the occurrence of oxygen usually cannot be detected from the isotopic pattern in routine spectra because the experimental error in relative intensities tends to be larger than the contribution of ^{18}O. Therefore, oxygen is frequently treated as an X type element although X + 2 would be a more appropriate but practically rather useless classification. In oligosaccharides, for instance, a substantial number of oxygen atoms contribute to the X + 2 signal.

Sulfur can be classified as an X + 2 element as long as only a few sulfur atoms are present in a molecule. However, the 0.8% contributed by ^{33}S to the X + 1 is almost comparable to the situation with ^{13}C (1.1% per atom). If the X + 1 peak is used for estimating the number of carbons present, then for ^{33}S this would cause an overestimation of the number of carbon atoms by roughly one carbon per sulfur (Fig. 3.10).

In the case of silicon the ^{30}Si isotope contributes a "mere" 3.4% to the X + 2 signal, and ^{29}Si even 5.1% to X + 1. So, neglecting ^{29}Si would cause an overestimation of the carbon number by 5 per Si present, which is unacceptable (Fig. 3.11).

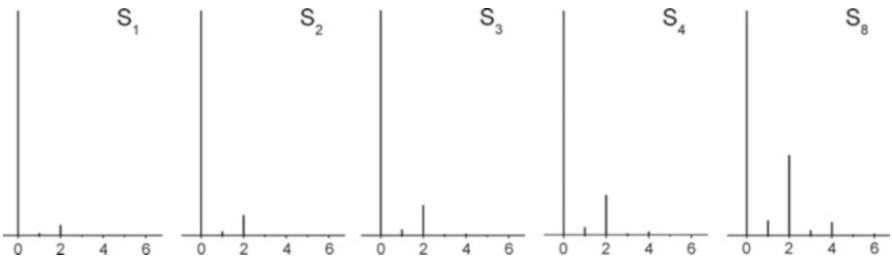

Fig. 3.10 Calculated isotopic patterns for combinations of elemental sulfur. The peak shown at zero position corresponds to the monoisotopic ion at *m*/*z* X. The isotopic peaks are then located at *m*/*z* = X + 1, 2, 3, ...

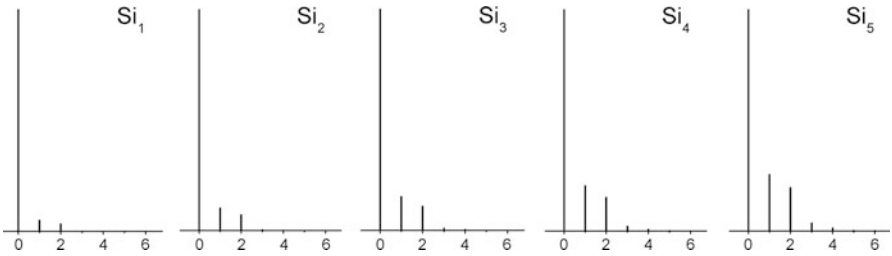

Fig. 3.11 Calculated isotopic patterns for combinations of elemental silicon. The peak shown at zero position corresponds to the monoisotopic ion at *m*/*z* X. The isotopic peaks are then located at *m*/*z* = X + 1, 2, 3, ...

Identifying S and Si

The presence of S and Si in a mass spectrum is best revealed by carefully examining the X + 2 intensity: this signal's intensity will be too high to be caused by the contribution of $^{13}C_2$ alone, even if the number of carbons has been obtained from X + 1 without prior subtraction of the S or Si contribution.

Isotopic pattern of a thioether The isotopic pattern calculated for ethyl propyl thioether, $C_5H_{12}S$, with the relative contributions of ^{33}S and ^{13}C to the M + 1 and of ^{34}S and $^{13}C_2$ to the M + 2 signal are shown below (Fig. 3.12 and Sect. 6.13). If the M + 1 peak resulted from ^{13}C alone, this would rather indicate the presence of 6 carbon atoms, which in turn would imply an M + 2 intensity of only 0.1% instead of the actually observed 4.6%. Consideration of Si for explaining the isotopic pattern would still fit the M + 2 intensity, however with relatively low accuracy, while for M + 1 the situation would be quite different. As ^{29}Si itself demands 5.1% at M + 1, there would be no or one carbon maximum allowed to explain the observed M + 1 intensity.

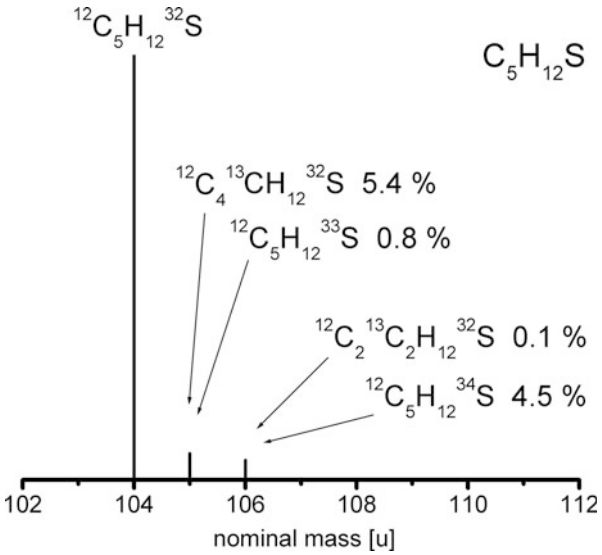

Fig. 3.12 Ethyl propyl thioether, $C_5H_{12}S$ – calculated isotopic pattern of the molecular ion indicating the respective contributions of ^{33}S and ^{13}C to the M + 1 and of ^{34}S and $^{13}C_2$ to the M + 2 signal

3.2.8 Polyisotopic Elements

The treatment of polyisotopic elements does not require other techniques as far as calculation or construction of isotopic patterns are concerned. However, isotopic patterns can differ largely from what has been considered so far and it is worth mentioning their peculiarities.

The polyisotopic element tin The presence or absence of tin, a polyisotopic element, can readily be detected from its characteristic isotopic pattern. For tetrabutyltin, $C_{16}H_{36}Sn$, the lowest mass isotopic composition is $^{12}C_{16}H_{36}{}^{112}Sn$, 340 u. Regarding the 16 carbon atoms, the ^{13}C isotopic abundance is about 17.5%. This is superimposed on the isotopic pattern of elemental Sn, which becomes especially obvious at 345 and 347 u (Fig. 3.13). The bars labeled with a tin isotope alone are almost solely due to $^{x}Sn^{12}C$ species. Tin neither has an isotope ^{121}Sn nor ^{123}Sn, and therefore the contributions at 349 and 351 u must be due to $^{120}Sn^{13}C$ and $^{122}Sn^{13}C$, respectively.

3.2.9 Practical Aspects of Isotopic Patterns

The recognition of isotopic patterns bears some potential pitfalls. Particularly, if signals from compounds differing by two or four hydrogens are superimposed or if such a superimposition can not a priori be excluded, the observed pattern has to be stepwise carefully checked to avoid misinterpretation of mass spectral data. When isotopically labeled compounds are involved similar care also becomes necessary.

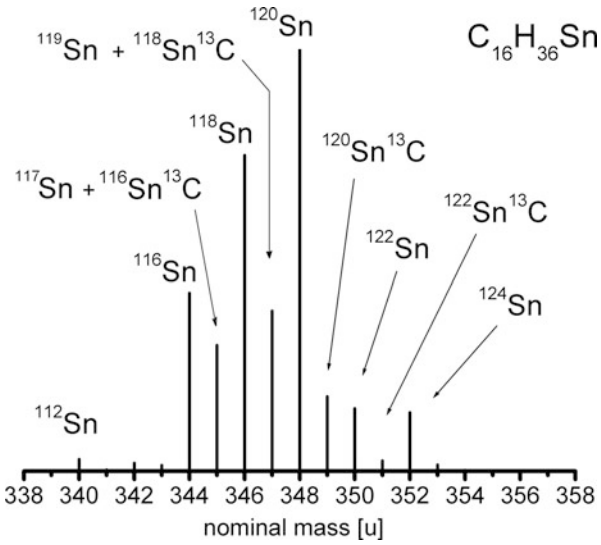

Fig. 3.13 Tetrabutyltin, $C_{16}H_{36}Sn$. Calculated isotopic pattern and isotopic compositions of the major contributions to the peaks

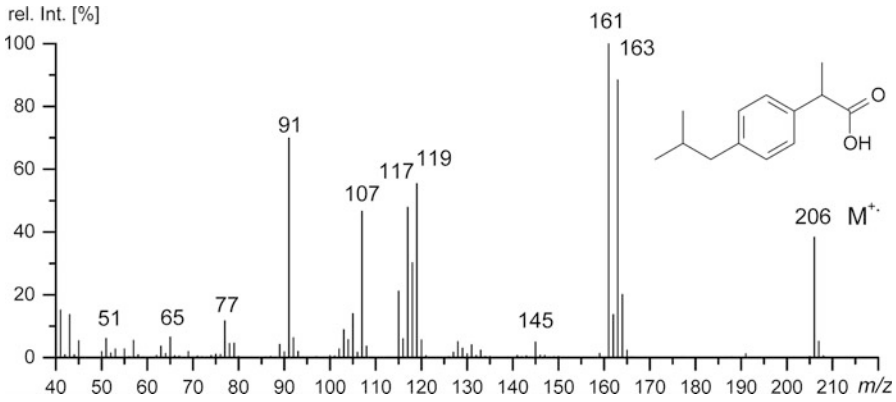

Fig. 3.14 EI mass spectrum of ibuprofen showing some signals that can be misinterpreted as a bromine isotopic pattern (Adapted with permission. © NIST, 2011)

A clear-cut bromine pattern! Or maybe not? The EI spectrum of ibuprofen shows some "fake" isotopic patterns. Supposing it to be an unknown, the peak pairs at *m*/*z* 161, 163 and also at *m*/*z* 117, 119 could easily be misinterpreted as isotopic patterns due to bromine, more exactly Br_1 (Fig. 3.14). However, a closer examination reveals that both pairs do not have the required intensity ratio of about 100 : 98. Instead, the peak at *m*/*z* 163 is merely at a relative intensity of 89% of *m*/*z* 161. In case of the *m*/*z* 117, 119 pair the intensity ratio is even reversed. Also, a look at the molecular ion peak at *m*/*z* 206 reveals that there is no bromine isotopic pattern at all.

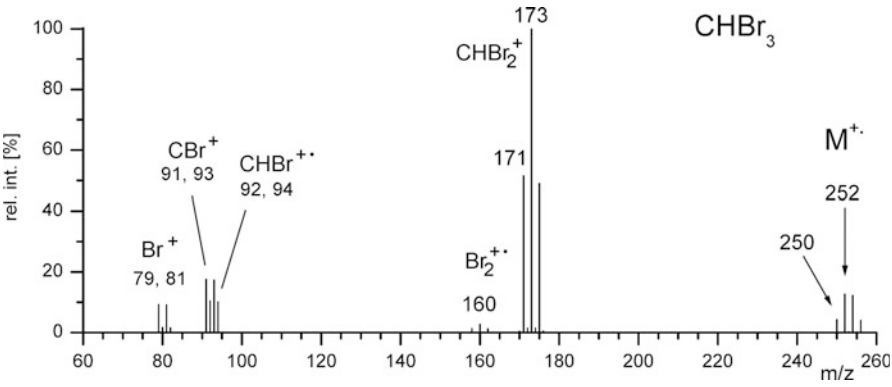

Fig. 3.15 Tribromomethane EI mass spectrum (Adapted with permission. © NIST, 2011)

If bromine was present, it necessarily had to cause the isotopic pattern for the $M^{+\bullet}$ ion, too. The true reason for ions of *m*/*z* 163 is loss of $C_3H_7^{\bullet}$, 43 u, from $M^{+\bullet}$ ions whereas ions at *m*/*z* 161 are due to a loss of $COOH^{\bullet}$, 45 u. Furthermore, there should be some peaks by Br^+ at *m*/*z* 79, 81 and by $HBr^{+\bullet}$, *m*/*z* 80, 82, which are absent, however. This case shows us that many patterns that superficially appear to be clear-cut and straight forward at first sight may require reinterpretation. Relative intensities need to be compared with tabulated data and all information of a spectrum needs to be considered.

3.2.10 Bookkeeping with Isotopic Patterns in Mass Spectra

Proving the identity of isotopic patterns requires careful comparison with calculated patterns. The mass differences must be consistent with the mass of the presumed neutral losses. In order to hold true, a pattern can only be assigned to signals at or above the mass given by the sum of all contributing atoms.

In calculating the mass differences between peaks from different isotopic patterns it is strongly recommended to proceed from the monoisotopic peak of one group to the monoisotopic peak of the next. Accordingly, the mass difference obtained also owes to the loss of a monoisotopic fragment. Otherwise, one bears the risk of erroneously omitting or adding hydrogens in a formula.

Tricky tribromomethane The EI mass spectrum of tribromomethane is dominated by the bromine isotopic distribution (Fig. 3.15). At first, there is no need to wonder *why* tribromomethane fragments like it does upon EI (Sect. 6.1). Let us simply accept this fragmentation and focus on the isotopic patterns. By referring to Fig. 3.5 one can identify the patterns of Br_3, Br_2, and Br. As a matter of fact, the molecular ion must contain the full number of bromine atoms (*m*/*z* 250, 252, 254, 256).

The primary fragment ion due to $Br^{\bullet}$ loss will then show a Br_2 pattern (*m*/*z* 171, 173, 175). A mass difference of 79 u is calculated between *m*/*z* 250 and *m*/*z*

171, owing to ^{79}Br, and thus identifying the process as a loss of $Br^{\bullet}$. Starting from the $CH^{79}Br_2{}^{81}Br$ isotopic ion at *m*/*z* 252 would yield the same information if ^{81}Br was used for the calculation. Here, ^{79}Br would wrongly indicate loss of H_2Br.

Subsequent elimination of HBr leads to CBr^+ at *m*/*z* 91, 93. Alternatively, the molecular ion can eliminate Br_2 to form $CHBr^{+\bullet}$, *m*/*z* 92, 94, overlapping with the *m*/*z* 91, 93 doublet, or it may lose CHBr to yield $Br_2{}^{+\bullet}$, causing the peaks at *m*/*z* 158, 160, 162. The peaks at *m*/*z* 79, 81 are due to Br^+ and those at *m*/*z* 80, 82 result from $HBr^{+\bullet}$ formed by CBr_2 loss from the molecular ion.

3.2.11 Information from Complex Isotopic Patterns

If the isotopic distribution is very broad and/or there are elements encountered that have a lowest mass isotope of very low abundance, recognition of the monoisotopic peak would become rather uncertain. However, there are ways to cope with that situation.

Find a checkpoint The ^{112}Sn isotopic peak of tin compounds can easily be overlooked or simply could be superimposed by background signals (Fig. 3.13). Here, one should identify the ^{120}Sn peak from its unique position within the characteristic pattern before screening the spectrum for Sn patterns from peak to peak. For all other elements contained in the respective ions still the lowest mass isotope would be used in calculations.

Assign a marker isotope Ruthenium exhibits a wide isotopic distribution of which the ^{102}Ru isotope can be used as a marker during assignment of mass differences. Moreover, the strong isotopic fingerprint of Ru makes it easily detectable from mass spectra and even compensates for a lack of information resulting from moderate mass accuracy (Fig. 3.16).

Refer to an abundant isotope
If the isotopic distribution is broad and/or there are elements encountered that have a lowest mass isotope of very low abundance, it is recommended to base calculations on the most abundant isotope of the respective element.

3.2.12 Systematic Approach to Reading Isotopic Patterns

Most mass spectra exhibit some sort of isotopic pattern. Especially those of organic molecules never come without at least a contribution from ^{13}C. It is thus good practice to carefully examine mass spectra for isotopic patterns, some of which may be obvious like those of Br and Cl, while others can be less apparent like those from Si, S, or Li, for example. When starting to interpret a mass spectrum, you are well

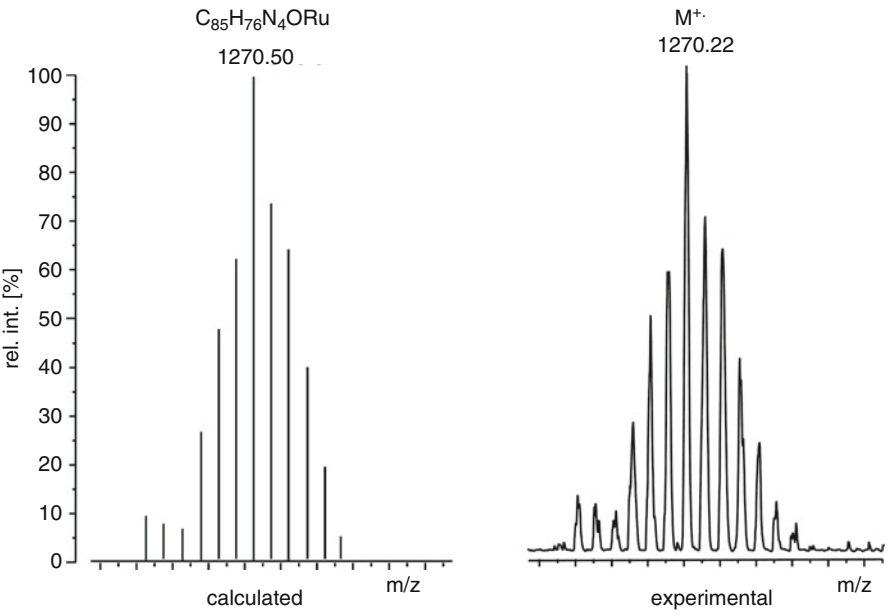

Fig. 3.16 Ruthenium carbonyl porphyrin complex – calculated and experimental isotopic pattern (FD-MS, cf. Sect. 8.6). The isotopic pattern supports the presumed molecular composition. The labeled peak corresponds to the ^{102}Ru-containing ion (Adapted from Ref. [28] with permission. © IM Publications, 1997)

advised to begin by carefully looking for isotopic patterns. A guideline is provided below (Fig. 3.17).

3.3 Isotopic Enrichment and Isotopic Labeling

3.3.1 Isotopic Enrichment

If the abundance of a particular nuclide is higher than the natural level in an ion, the term *isotopically enriched ion* is used to describe any ion enriched in the isotope [4]. The degree of *isotopic enrichment* is best determined by mass spectrometry.

Fullerenes enriched in ^{13}C Isotopic enrichment is a standard means to enhance the response of an analyte in nuclear magnetic resonance (NMR). Such measures gain importance if extremely low solubility is combined with a large number of carbons, as is often the case with [60]fullerene compounds [29]. The molecular ion signals, $M^{+\bullet}$, of C_{60} with natural isotopic abundance and of ^{13}C–enriched C_{60} are shown below (Fig. 3.18); for EI-MS of [60]fullerenes cf. Refs. [30–32]). From these mass spectra, the ^{13}C enrichment can be determined by use of Eq. (3.2). For C_{60} of natural isotopic abundance we obtain $M_{rC60} = 60 \times 12.0108\ \text{u} = 720.65\ \text{u}$. Applying

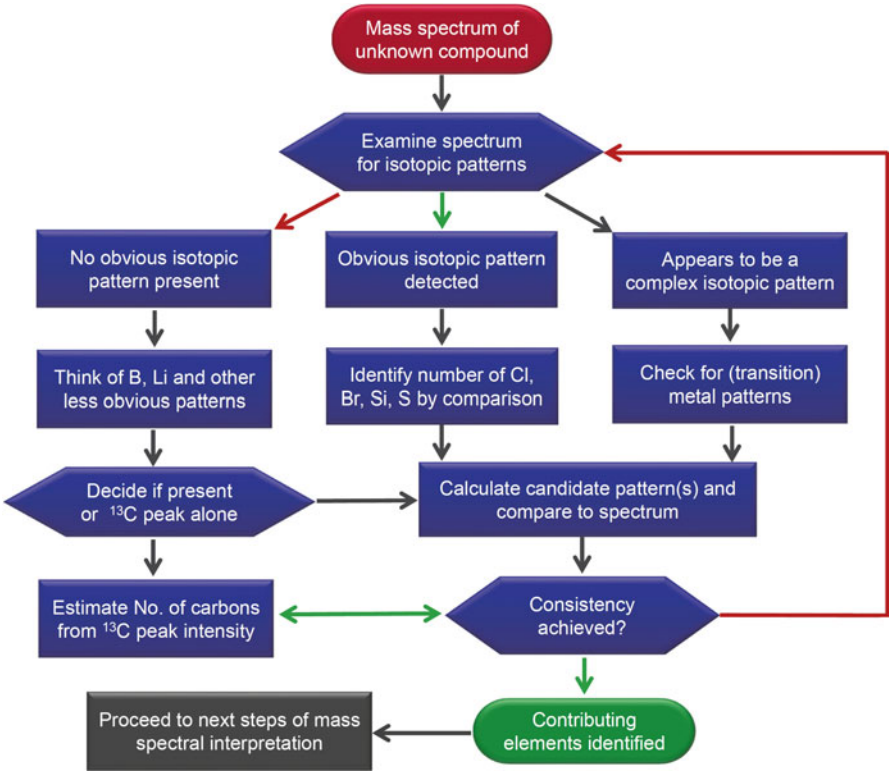

Fig. 3.17 Guideline for the identification of contributing elements based on isotopic pattern analysis

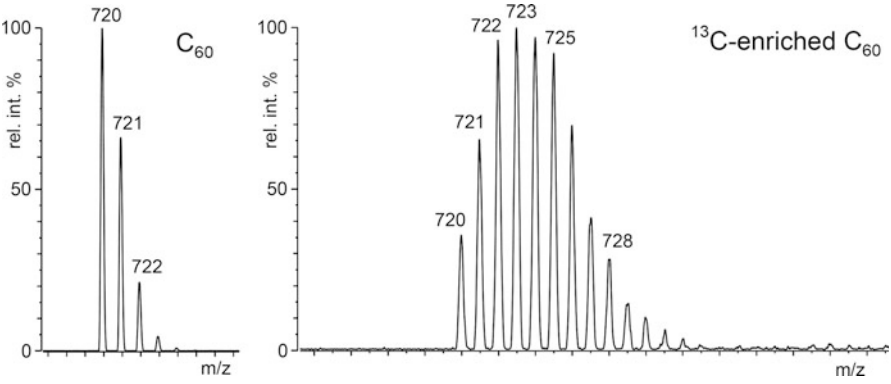

Fig. 3.18 [60]Fullerene – comparison of the molecular ion signals, $M^{+\bullet}$, with natural isotopic abundance and of ^{13}C–enriched C_{60} (By courtesy of W. Krätschmer, Max Planck Institute for Nuclear Physics, Heidelberg)

Eq. (3.2) to the isotopically enriched compound yields $M_{r13C\text{-}C60} = (35 \times 720 + 65 \times 721 + 98 \times 722 + 100 \times 723 + 99 \times 724 + 93 \times 725 + ...)$ u/$(35 + 65 + 98 + 100 + 99 + 93 + ...) = 724.10$ u. (Integer mass and intensity values are used here for clarity.) This result is equivalent to an average content of 4.1 ^{13}C atoms per [60]fullerene molecule which on the average means 3.45 ^{13}C atoms more than the natural content of 0.65 ^{13}C atoms per molecule.

3.3.2 Isotopic Labeling

If the abundance of a particular nuclide is higher than the natural level at one or more (specific) positions within an ion, the term *isotopically labeled ion* is used to describe such an ion. Among other applications, *isotopic labeling* is used in order to track metabolic pathways, to serve as internal standard for quantitative analysis, or to elucidate fragmentation mechanisms of ions in the gas phase. In mass spectrometry, the nonradiating isotopes ^{2}H (deuterium, D), ^{13}C, and ^{18}O are preferably employed and thus, a rich methodology to incorporate isotopic labels has been developed [33]. Isotopic labeling is rather a mass spectrometric research tool [34] than mass spectrometry being a tool to control the quality of isotopic labeling. As a result, isotopic labeling is used in many applications; examples are given throughout the book.

3.4 Resolution and Resolving Power

3.4.1 Definitions

So far, we have taken for granted that mass spectra separate isotopic patterns; now we want to quantify this degree of separation. The separation observed in a mass spectrum is termed *mass resolution*, R, or simply *resolution* [35]. Mass resolution is given as the smallest difference in m/z , i.e., $\Delta(m/z)$ that can be separated for a given signal, i.e., at a given m/z value:

$$R = \frac{m}{\Delta m} = \frac{m/z}{\Delta(m/z)} \tag{3.11}$$

Accordingly resolution is dimensionless. The ability of an instrument to resolve neighboring peaks is called its *mass resolving power* or simply *resolving power*. It is obtained from the peak width at a specific percentage of the peak height expressed as a function of mass [4, 35].

Two neighboring peaks are assumed to be sufficiently separated when the valley separating their maxima has decreased to 10% of their intensity. Hence, this is known as *10% valley definition of resolution*, $R_{10\%}$. The 10% valley conditions are fulfilled if the peak width at 5% relative height equals the mass difference of the corresponding ions, because then the 5% contribution of each peak to the same point of the m/z axis adds up to 10% (Fig. 3.19).

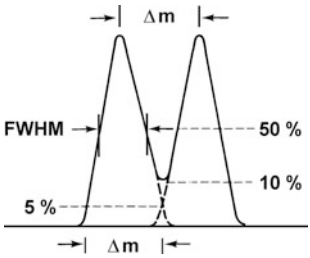

Fig. 3.19 The 10% valley and full width at half maximum (FWHM) definitions of resolution. Peak heights are not to scale

With the advent of linear quadrupole analyzers the *full width at half maximum* (*FWHM*) *definition* of resolution became widespread especially among instruments manufacturers. It is also commonly used for time-of-flight and quadrupole ion trap mass analyzers. With Gaussian peak shapes, the ratio of R_{FWHM} to $R_{10\%}$ is 1.8. The resolution for a pair of peaks at different m/z and its practical implications are illustrated below (Fig. 3.20).

Resolution affects spectrum of residual air The changes in the electron ionization spectra of residual air nicely show the effect of higher resolution (Fig. 3.21). Setting $R = 1000$ yields a peak width of 0.028 u for the signal at m/z 28. An increase to $R = 7000$ perfectly separates the minor contribution of CO^+, m/z 27.995, from the predominating $N_2^{+\bullet}$ at m/z 28.006 (The CO^+ ion rather results from fragmenting $CO_2^{+\bullet}$ ions than from carbon monoxide in laboratory air.)

LR and HR
The attributive *low resolution* (LR) is generally used to describe spectra obtained at $R < 3000$. *High resolution* (HR) is appropriate for $R > 5000$. However, there is no exact definition of these terms.

3.4.2 Resolution and Its Experimental Determination

In principle, resolution is always determined from the peak width of some signal at a certain relative height and therefore, any peak can serve this purpose. As the exact determination of a peak width is not always easy to perform, certain doublets of known Δm are being used.

The minimum resolution to separate CO^+ from $N_2^{+\bullet}$ is $28/0.011 \approx 2500$. The doublet from the pyridine molecular ion, $C_5H_5N^{+\bullet}$, m/z 79.0422, and from the first isotopic peak of the benzene molecular ion, $^{13}CC_5H_6^{+\bullet}$, m/z 79.0503, necessitates $R = 9750$ to be separated. Finally, the doublet composed of the first isotopic ion of $[M–CH_3]^{+\bullet}$ from xylene, $^{13}CC_6H_7^+$, m/z 92.0581, and toluene molecular ion, $C_7H_8^{+\bullet}$, m/z 92.0626, requires $R = 20{,}600$ for separation (Fig. 3.22).

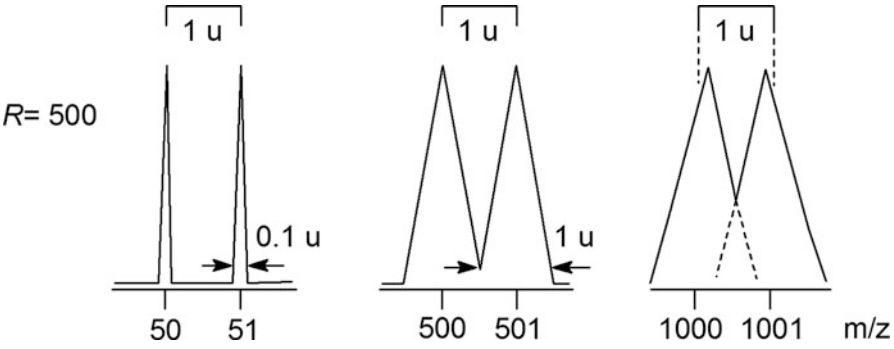

Fig. 3.20 Simulated signals of simplified triangular shape at *m*/*z* 50, 500, and 1000 as obtained at $R = 500$. At *m*/*z* 1000 the peak maxima shift towards each other due to superimposing peaks; this also approximates the result of $R_{FWHM} = 900$

Report resolution rounded
There is no need to use a more accurate value of *m*/*z* than nominal and likewise, there is no use of reporting $R = 2522.52$ exactly as obtained for the $CO^+/N_2^{+\bullet}$ pair. It is fully sufficient to know that setting $R = 3000$ is sufficient for one specific task or that $R = 10{,}000$ is suitable for another.

With magnetic sector instruments a resolving power of up to $R = 10{,}000$ can routinely be employed, even $R = 15{,}000$. In practice, those instruments are rarely adjusted to resolve beyond $R = 10{,}000$, e.g., only when interferences of ions of the same nominal *m*/*z* need to be excluded. With an instrument in perfect condition, it is possible to achieve higher resolving power; typically they are specified to deliver about $R \approx 60{,}000$ (on intensive peaks).

3.4.3 Resolving Power and Its Effect on Relative Peak Intensity

Increasing resolution does not affect the relative intensities of the peaks, i.e., the intensity ratios for *m*/*z* 28 : 32 : 40 : 44 in the spectrum of air generally remain constant (Fig. 3.22). However, increased settings of resolving power are often obtained at the cost of transmission of the mass analyzer, thereby reducing the absolute signal intensity. Accordingly, isotopic patterns are not affected by increasing resolution up to $R \approx 10{,}000$; beyond, there can be changes in isotopic patterns due to the separation of different isotopic species of the same nominal mass (Sect. 3.7).

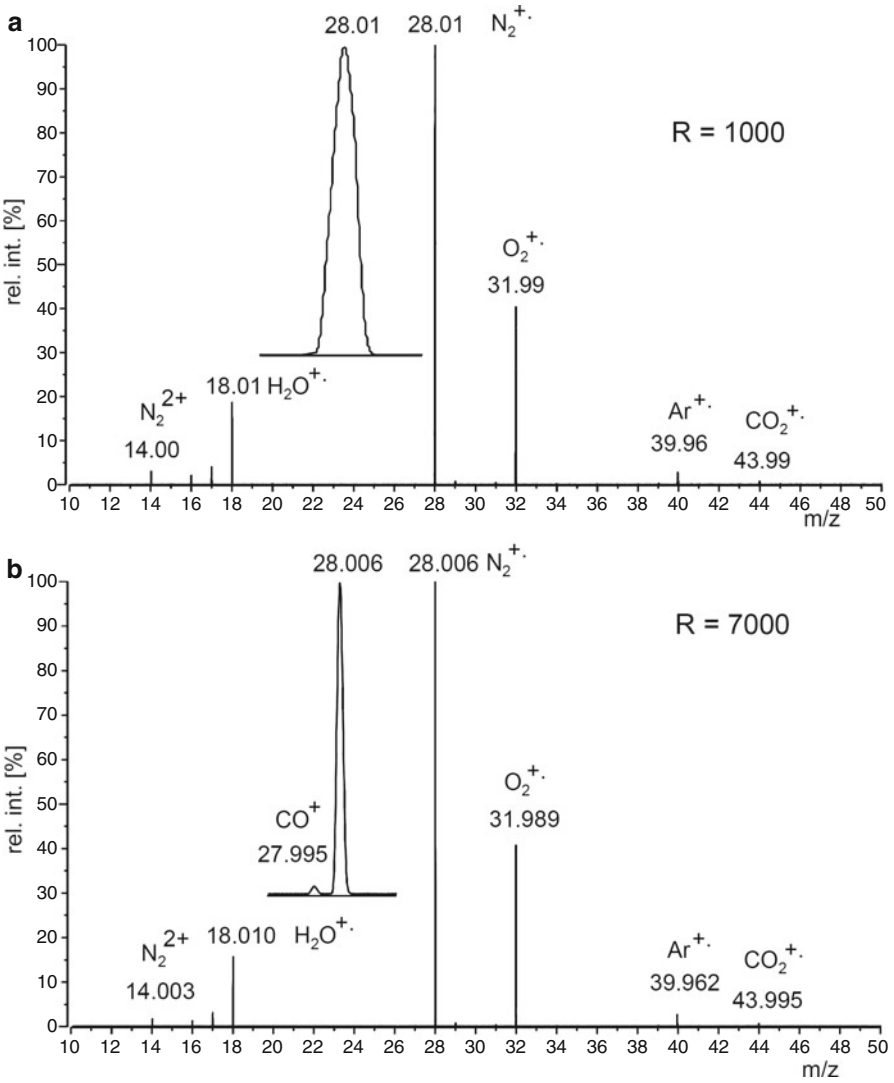

Fig. 3.21 EI mass spectra of residual air (**a**) at $R = 1000$ and (**b**) at $R = 7000$. The relative intensities are not affected by different resolution. The decimal digits of the mass labels indicate achievable mass accuracies under the respective conditions

3.5 Accurate Mass

The section on high resolution (HR) already anticipated *accurate mass* to a certain extent. In fact, HR and accurate mass measurements are closely related and depend on each other, because mass accuracy tends to improve as peak resolution is

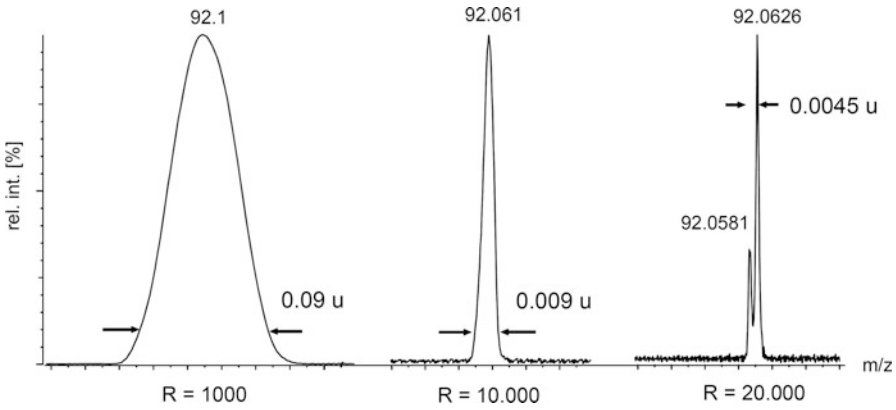

Fig. 3.22 The *m*/*z* 92 peak from a mixture of xylene and toluene at different resolving power. At $R = 10{,}000$ some separation of the lower mass ion can already be presumed from a slight asymmetry of the peak. $R = 20{,}600$ is needed to fully separate $^{13}CC_6H_7^+$, *m*/*z* 92.0581, from $C_7H_8^{+\bullet}$, *m*/*z* 92.0626. The *m*/*z* scale is the same for all of the signals

improved. Nevertheless, they should not be confused, as performing a measurement at *high resolution* alone does not equally imply measuring the *accurate mass*. High resolution separates adjacent signals, accurate mass can deliver molecular formulas [36–38].

Until the early 1980s, accurate mass measurements were nearly restricted to electron ionization, and for a while, the technique even seemed to become abandoned. New options available through FT-ICR instrumentation then revived the value of accurate mass measurements. The newly developed Orbitrap and a new generation of oaTOF analyzers contributed to an increased demand for accurate mass data. Nowadays, formula elucidation can be performed using any ionization method [39], their widespread application thus demanding a thorough understanding of their potential and limitations [37].

3.5.1 Exact Mass and Molecular Formulas

Let us briefly summarize some important definitions and terms related to ionic mass:

- The *isotopic mass* is the *exact mass* of an isotope.
- The isotopic mass is very close but not equal to the *nominal mass* of that isotope.
- The calculated exact mass of a molecule or of a monoisotopic ion equals its monoisotopic mass.
- The definition of our mass scale will imply that the isotope ^{12}C represents the only exception from non-integer isotopic mass.

As a consequence of these individual non-integer isotopic masses, no combination of elements in a molecular or ionic formula has the same *calculated exact mass*, or simply *exact mass* as it is often referred to, as any other one [40]. In other words, any elemental composition has its unique exact mass. Infinite accuracy provided, any formula can be identified by the accurate mass of the ions.

Isobaric ions of *m/z* 28 The molecular ions of nitrogen, $N_2^{+\bullet}$, carbon monoxide, $CO^{+\bullet}$, and ethene, $C_2H_4^{+\bullet}$, have the same nominal mass of 28 u, i.e., they are so-called *isobaric ions*. The isotopic masses of the most abundant isotopes of hydrogen, carbon, nitrogen, and oxygen are 1.007825 u, 12.000000 u, 14.003074 u, and 15.994915 u, respectively. Thus, the calculated ionic masses are 28.00559 u for $N_2^{+\bullet}$, 27.99437 u for $CO^{+\bullet}$, and 28.03075 u for $C_2H_4^{+\bullet}$. This means they differ by several 10^{-3} u, and none of these isobaric ions has precisely 28.00000 u (Sects. 3.1.5 and 6.10.6).

The "mmu"
Historically, 10^{-3} u was referred to as 1 *millimass unit* (mmu). There is still some use of mmu in the MS community because of its convenience in dealing with small differences in mass. However, using the SI prefix m for milli, the correct way of writing 10^{-3} u would be as 1 mu or 1 mDa (non IUPAC).

3.5.2 Relativistic Mass Defect

Mass–energy equivalence is a key postulate of Einstein's theory of relativity as expressed by his famous eq. $E = mc^2$. It describes the conversion of mass into energy during nucleation. The binding energy per nucleon steeply increases along the mass numbers from ^{2}H to its maximum around ^{56}Fe and then decreases again somewhat up to ^{238}U (Fig. 3.23). Translation into isotopic mass reveals that mass is by some 10^{-3} u above the nominal value for light elements (^{1}H, ^{4}He, ^{7}Li, ^{11}B, ^{14}N), while being some 10^{-3} u (^{19}F) to almost 10^{-1} u (^{127}I) below that for heavier elements [38]. This also complies with the fact that the radioactive isotopes of thorium and uranium have isotopic masses above the nominal value, thus reflecting their comparatively unstable nuclei (Appendix).

3.5.3 Role of Mass Defect in Mass Spectrometry

The term *mass defect*, m_{defect}, is defined as the difference between integer mass, m_{nominal}, and exact mass, m_{exact}, and is used to describe this deviation [6].

$$m_{\text{defect}} = m_{\text{nominal}} - m_{\text{exact}} \tag{3.12}$$

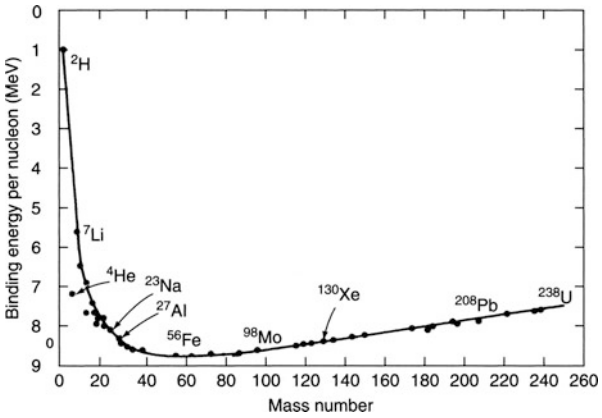

Fig. 3.23 Plot of binding energy per nucleon vs. mass number (Reproduced from Ref. [1] by permission. © John Wiley & Sons, 1992)

Application of this concept leads to *positive* and *negative mass* defects. The hydrogen atom, for example, has a negative mass defect, $m_{\text{defectH}} = -7.825 \times 10^{-3}$ u. In addition, the assumption that things appearing to be "defective" are associated with certain isotopic masses can be misleading. The mass defect was unveiled by Aston [2, 3] who already had discovered 212 of the total 287 stable isotopes. Obviously, the deviation of exact mass from nominal mass can be either to the higher or lower side, depending on the isotopes encountered. While the issue itself is easy to understand, the current terminology here can be somewhat deceptive.

The term *mass deficiency* better describes the fact that the exact mass of an isotope or a complete molecule is lower than the corresponding nominal mass. In case of ^{16}O, for example, the isotopic mass is 15.994915 u, being 5.085×10^{-3} u deficient as compared to the nominal value ($m_{\text{defectO}} = 5.085 \times 10^{-3}$ u). Most isotopes are more or less mass deficient with a tendency towards larger mass defect for the heavier isotopes, e.g., $M_{35\text{Cl}} = 34.96885$ u (-3.115×10^{-2} u) and $M_{127\text{I}} = 129.90447$ u (-9.553×10^{-2} u).

Among the elements frequently encountered in mass spectrometry, only H, He, Li, Be, B, and N exhibit isotopic masses larger than their nominal value. Among the isotopes with negative mass defect, ^{1}H is the most important one, because each hydrogen adds 7.825×10^{-3} u. Thereby, it significantly contributes to the mass of larger hydrocarbon molecules [41]. In general, the ubiquitous occurrence of hydrogen in organic molecules causes most of them to exhibit considerable negative mass defects, which again decreases with the number of mass-deficient isotopes, e.g., from halogens, oxygen, or metals.

Mass deficiency as first indication Plotting the deviations from nominal mass of different oligomers as a function of nominal mass, one finds only pure carbon molecules (such as fullerenes) to be located on the *x*-axis. Hydrocarbons, due to their large number of hydrogens, receive roughly 1 u from negative mass defect per 1000 u in molecular mass. Halogenated oligomers, on the other hand, are more or

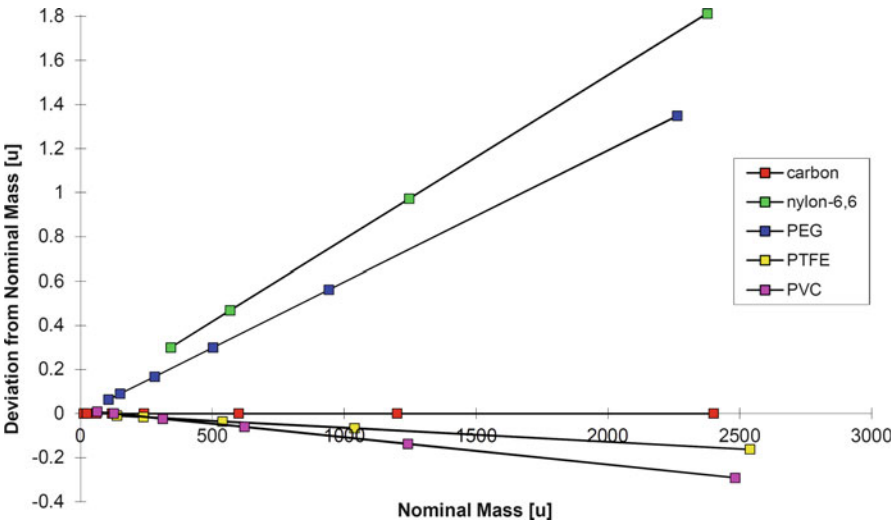

Fig. 3.24 Deviation from nominal mass for some oligomers as a function of nominal mass. *PE* polyethylene, *PEG* polyethyleneglycol, *PTFE* polytetrafluoroethylene, *PVC* polyvinylchloride

less mass deficient and those oligomers containing some oxygen are located in between (Fig. 3.24).

Limits of nominal mass
The use of nominal mass is limited to the low mass range. Above about 400–500 u the first decimal of isotopic mass can be larger than 0.5 causing it to be rounded up, e.g., to 501 u instead of the expected value of 500 u. This, in turn, will lead to severe misinterpretation of a mass spectrum (Chap. 6). One should write m/z values above m/z 400 with at least one decimal, e.g., as m/z 474.5 for $[C_{34}H_{66}]^{+\bullet}$.

3.5.4 Mass Accuracy

The *absolute mass accuracy*, $\Delta(m/z)$, is defined as the difference between *measured accurate mass* and *calculated exact mass*:

$$\Delta(m/z) = m/z_{\text{experimental}} - m/z_{\text{calculated}} \tag{3.13}$$

Instead of stating the absolute mass accuracy in units of u, it can also be given as *relative mass accuracy*, $\delta m/m$, i.e., absolute mass accuracy divided by the mass it is determined for:

$$\delta m/m = \Delta(m/z)/(m/z) \tag{3.14}$$

The *relative mass accuracy*, $\delta m/m$, is normally given in *parts per million* (ppm). As mass spectrometers tend to have similar absolute mass accuracies over a comparatively wide range, absolute mass accuracy represents a more meaningful way of stating mass accuracies than the use of ppm.

Use of ppm and ppb
Part per million (1 ppm $= 10^{-6}$) is simply a relative measure as are percent (%) or permill (parts per thousand, ‰). In addition, *parts per billion* (1 ppb $= 10^{-9}$), and *parts per trillion* (1 ppt $= 10^{-12}$) are in use.

Accuracy or just the impression thereof A magnetic sector mass spectrometer allows for an absolute mass accuracy of $\Delta(m/z) = 0.002$–0.005 u in scanning mode over a range of about m/z 50–1500. At m/z 1200 an error of $\Delta(m/z) = 0.003$ u corresponds to inconspicuous $\delta m/m = 2.5$ ppm, whereas the same error yields 60 ppm at m/z 50, which appears to be unacceptably high.

3.5.5 Accuracy and Precision

The concepts of *accuracy* and *precision* can best be illustrated using the analogy to a target where the center represents the true value of some physical quantity [42]. Accuracy describes the deviation of the experimental value from the true value, which normally is rather an accepted reference value than a "true" one in the strict sense. Accuracy is high (A+ in Fig. 3.25) if the values from several measurements are close to the reference value. Accuracy depends on systematic errors of an experiment. Precision describes the deviation within a group of determinations and it is high (P+ in Fig. 3.25) if the values from several measurements are in close proximity to but not necessarily identical with the reference value. Precision is an expression of random error, e.g., as introduced by noise, variation in injection volumes or times. *Repeatability* and *reproducibility* are two aspects of precision. Repeatability is connected to the repetition of the same measurement on the same setup within a short time frame while reproducibility is related to long term stability of a setup and inter-platform or inter-operator effects. Suitable statistical evaluation of a widespread dataset can result in an accurate determination of a quantity at the cost of lower precision (P– A?), e.g., root-mean-square deviation (Sect. 3.6.4) [43, 44].

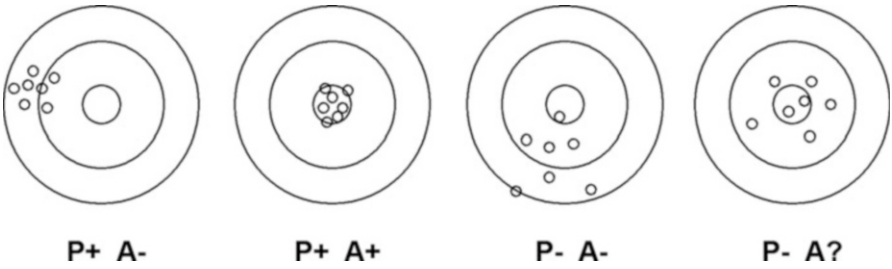

Fig. 3.25 Precision (*P*) and accuracy (*A*), along with seven hits on a target

3.5.6 Mass Accuracy and the Determination of Molecular Formulas

Assuming infinite mass accuracy, we should be able to identify the molecular formula of any ion merely on the basis of its exact mass – the emphasis is on *infinite* mass accuracy (Sect. 3.5.1). In reality we are dealing with errors in the order of one to several ppm depending on the type of instrument and the mode of its operation.

Number of formulas to be considered The number of possible even-electron ionic formulas based on an unrestricted selection among the elements C, H, N, and O as a function of relative mass error strongly depends on the *m*/*z* value of the ion. Here, the formulas proposed for the measured signals from $[(\text{arginine})_{1–5} + \text{H}]^+$ cluster ions, *m*/*z* 175.1189, 349.2309, 523.3427, 697.4548, and 871.5666 were counted for different relative mass error. While the lowest-mass ion is undoubtedly identified up to 5 ppm, the second ion is only unambiguously identified up to 2 ppm (Fig. 3.26). Allowing sulfur ($S_{0–2}$) in addition would already result in 18 rather than the 7 hits shown for the $[(\text{arginine})_3 + \text{H}]^+$ ion, *m*/*z* 523.3427, at 2 ppm error. Taking also odd-electron ions into account would contribute another 15 compositions to this selection. In case of the $[(\text{arginine})_5 + \text{H}]^+$ ion, *m*/*z* 871.5666, the number of C, H, N, O hits reaches 26 at 1 ppm error and even 232 at 10 ppm.

Unequivocal formula assignment by accurate mass alone only works in a range up to about *m*/*z* 500 depending on the particular restrictions [45]. Obviously, for ions of larger *m*/*z* the number of hits rapidly increases beyond a reasonable limit. Even at a high mass accuracy of 1 ppm and with the particular case of peptides the elemental composition can only be unambiguously identified up to about 800 u [46–48]. Determining the formula of a peptide among all natural peptide compositions possible at *m*/*z* 1005.4433 requires $\delta m/m = 0.1$ ppm [49].

The situation becomes more complicated as more elements and fewer limitations of their number must be taken into account. In practice, one must try to restrict oneself to certain elements and a maximum and/or minimum number of certain isotopes to assure a high degree of confidence in the assignment of formulas. Isotopic patterns provide a prime source of such additional information. Combining the information from accurate mass data and experimental peak intensities with

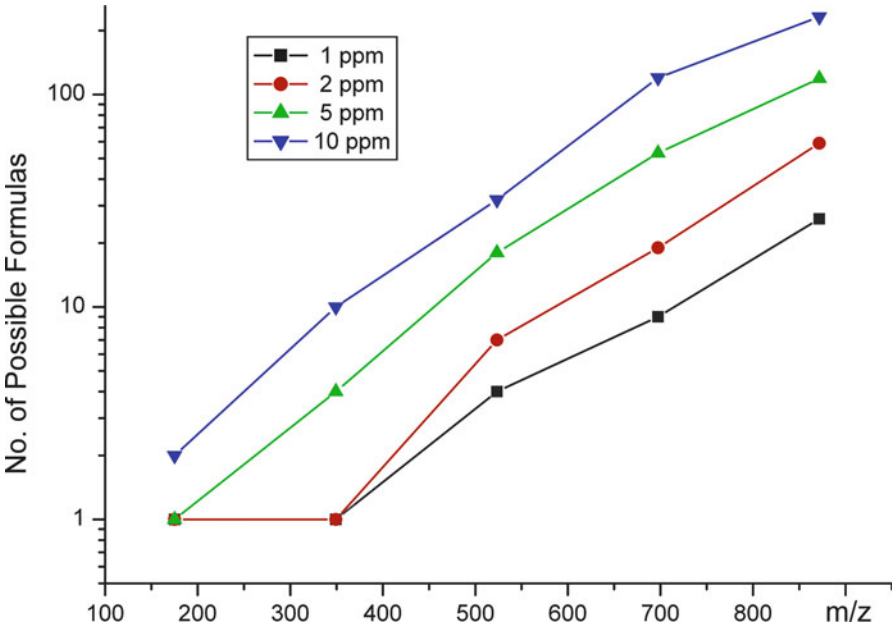

Fig. 3.26 Number of possible even-electron ionic formulas based on a free selection among the elements C, H, N, O as a function of relative mass error vs. *m*/*z*. The data points correspond to $[(\text{arginine})_{1-5} + \text{H}]^+$ cluster ions, *m*/*z* 175.1189, 349.2309, 523.3427, 697.4548, and 871.5666. The lines are meant as visual guides

calculated isotopic patterns allows to significantly reduce the number of potential elemental compositions of a particular ion [50, 51].

3.5.7 Extreme Mass Accuracy: Special Considerations

Even when we have determined a molecular formula, it does not tell us much about the structure of the molecule. According to the mass–energy equivalence (1 u = 931.5 MeV), a mass accuracy of 1 ppm ($\delta m/m = 10^{-6}$) roughly corresponds to an energy of 100 keV if an ion of *m*/*z* 100 is considered. A mass accuracy of 1 ppb ($\delta m/m = 10^{-9}$) still corresponds to an energy of 100 eV, and thus, 1 ppt ($\delta m/m = 10^{-12}$) would be required to approach energy differences of 0.1 eV, i.e., between isomers. Obviously, isomers are (almost) perfect isobars [52]. Nonetheless, it is worth noting that physicist are approaching 10 ppt, at least in the case of single atomic species (Fig. 3.27).

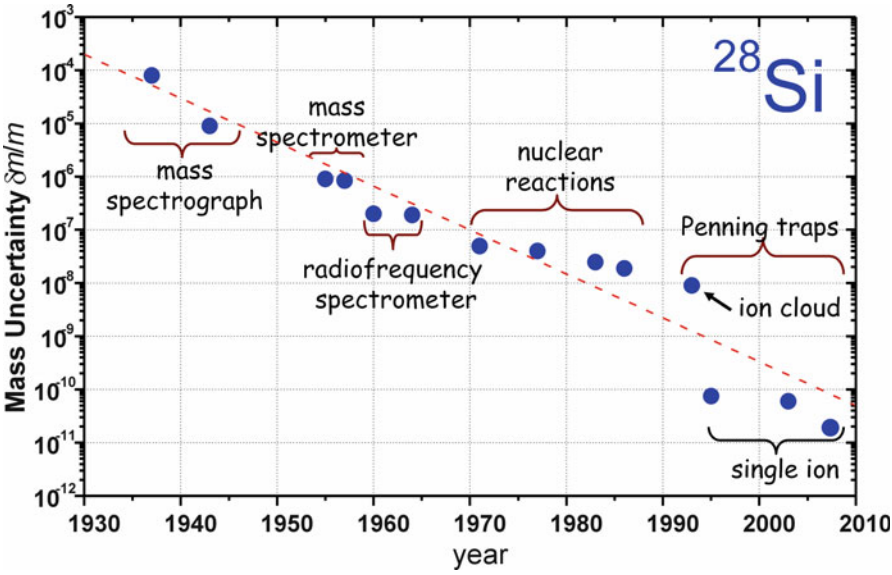

Fig. 3.27 Relative mass uncertainty $\delta m/m$ for ^{28}Si as a function of time. The most accurate mass of ^{28}Si so far is $m_{(28Si)} = 27.876926534\ 96(62)$ u corresponding to an uncertainty of 0.2 ppt. The *dashed line* serves as a visual orientation and reveals an improvement in accuracy by about one order of magnitude per decade (By courtesy of H.-J. Kluge, GSI Helmholtz Centre for Heavy Ion Research GmbH, Darmstadt, Germany)

3.6 Applied High-Resolution Mass Spectrometry

Generally, *high-resolution mass spectrometry* (HR-MS) aims to achieve both high mass resolution and high mass accuracy. These quantities have been introduced without considering the means by which they can be measured. The key to this problem is *mass calibration*. Resolution alone can separate ions with m/z in close proximity, but it does not automatically reveal where on the m/z axis the respective signals are located. This section deals with the techniques for establishing accurate mass data and their analytical evaluation [36, 37].

3.6.1 Mass Calibration

All mass spectrometers require *mass calibration* before they are put to use. However, proper procedures and the number of required calibration points may largely differ between different types of mass analyzers. Typically, a robust mass calibration necessitates several peaks of well-known m/z values evenly distributed over the mass range of interest. These are supplied from a well-known *mass calibration compound* or *mass reference compound*.

3.6.1.1 Compiling Mass Reference Lists

A mass reference list can be compiled once the mass spectrum of a calibration standard is known and the elemental composition of the ions that are to be included in the mass reference list are established by an independent measurement. For this purpose, the listed reference masses should be calculated down to six decimals. Otherwise, one runs a chance of obtaining erroneous reference values, especially when masses of ion series are calculated by multiplication of a subunit. This can easily be done using conventional spreadsheet applications.

Cluster ions as mass reference Cluster ions are frequently employed for mass calibration as they provide series of ions that are equidistant on the *m*/*z* axis [53–58]. For example, CsI and CsI_3, respectively, can be used for mass calibration in fast atom bombardment (FAB, Chap. 10) and matrix-assisted laser desorption/ionization (MALDI, Chap. 11) mass spectrometry because they yield cluster ions of the general formula $[Cs(CsI)_n]^+$ in positive-ion and $[I(CsI)_n]^-$ in negative-ion mode.

3.6.2 Performing an External Mass Calibration

Mass calibration is performed by recording a mass spectrum of the *calibration compound* and subsequent correlation of experimental *m*/*z* values to the *mass reference list* [37, 59, 60]. Usually, this conversion of the mass reference list to a calibration is accomplished by the mass spectrometer's software. Thus, the mass spectrum is recalibrated by interpolation of the *m*/*z* scale between the assigned calibration peaks to obtain the best match. The mass calibration obtained may then be stored in a *calibration file* and used for future measurements without the presence of a calibration compound. This procedure is termed *external mass calibration*.

The numerous ionization methods and mass analyzers in use have created a demand for a large number of calibration compounds to suit their specific needs. Therefore, mass calibration will variously be addressed at the end of the chapters on ionization methods.

Classical standard PFK *Perfluorokerosene* (PFK) is a well-established mass calibration standard in electron ionization. It provides evenly spaced $C_xF_y^+$ fragment ions over a wide mass range (Figs. 3.28 and 3.29). The major ions are all mass deficient, with CHF_2^+, *m*/*z* 51.0046, being the only exception. PFK mixtures are available from low-boiling to high-boiling grades which may be used up to *m*/*z* 700–1100. Apart from the highest boiling grades, PFK is suitable to be introduced by the reference inlet (Sect. 5.2.1), a property making it very attractive for internal calibration as well.

Calibration with perfluorotributylamine Perfluorotributylamine (PFTBA, also termed FC-43), is another frequently used calibrant in EI-MS. This single

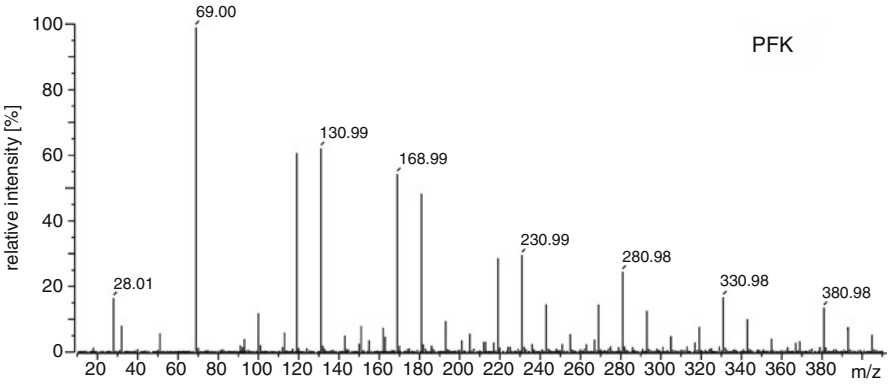

Fig. 3.28 Perfluorokerosene, PFK: partial 70-eV EI mass spectrum. The peaks are evenly distributed over a wide *m*/*z* range. Also, peaks from residual air occur in the low *m*/*z* range

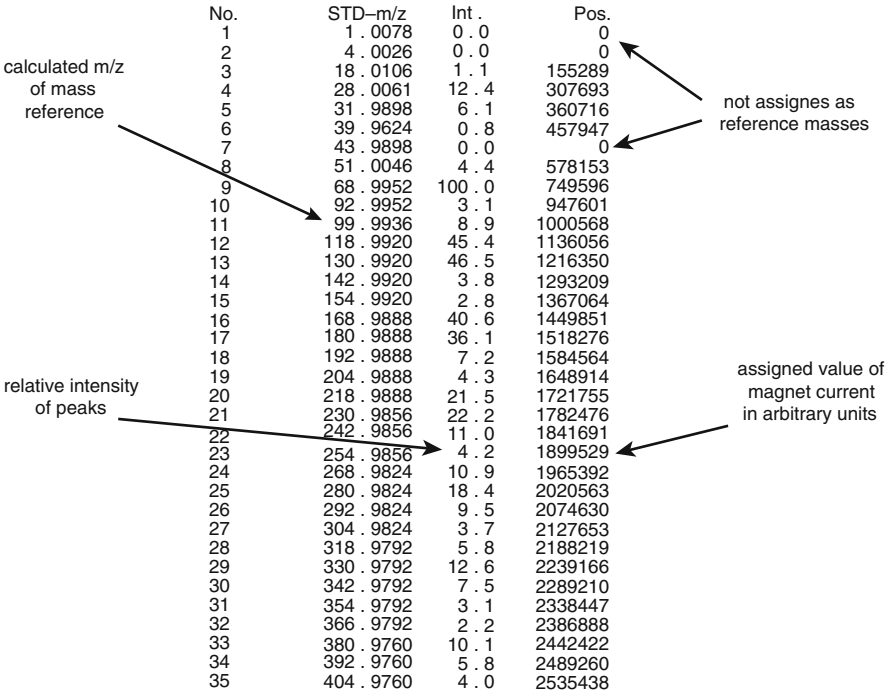

No.	STD–m/z	Int.	Pos.
1	1.0078	0.0	0
2	4.0026	0.0	0
3	18.0106	1.1	155289
4	28.0061	12.4	307693
5	31.9898	6.1	360716
6	39.9624	0.8	457947
7	43.9898	0.0	0
8	51.0046	4.4	578153
9	68.9952	100.0	749596
10	92.9952	3.1	947601
11	99.9936	8.9	1000568
12	118.9920	45.4	1136056
13	130.9920	46.5	1216350
14	142.9920	3.8	1293209
15	154.9920	2.8	1367064
16	168.9888	40.6	1449851
17	180.9888	36.1	1518276
18	192.9888	7.2	1584564
19	204.9888	4.3	1648914
20	218.9888	21.5	1721755
21	230.9856	22.2	1782476
22	242.9856	11.0	1841691
23	254.9856	4.2	1899529
24	268.9824	10.9	1965392
25	280.9824	18.4	2020563
26	292.9824	9.5	2074630
27	304.9824	3.7	2127653
28	318.9792	5.8	2188219
29	330.9792	12.6	2239166
30	342.9792	7.5	2289210
31	354.9792	3.1	2338447
32	366.9792	2.2	2386888
33	380.9760	10.1	2442422
34	392.9760	5.8	2489260
35	404.9760	4.0	2535438

Fig. 3.29 Reproduction of a partial PFK calibration table (*m*/*z* 1–305 range) of a magnetic sector instrument. In order to expand the PFK reference peak list to the low *m*/*z* range, ^{1}H, ^{4}He, and peaks from residual air are included, but for intensity reasons ^{1}H, ^{4}He, and CO_2 have not been assigned in this particular case

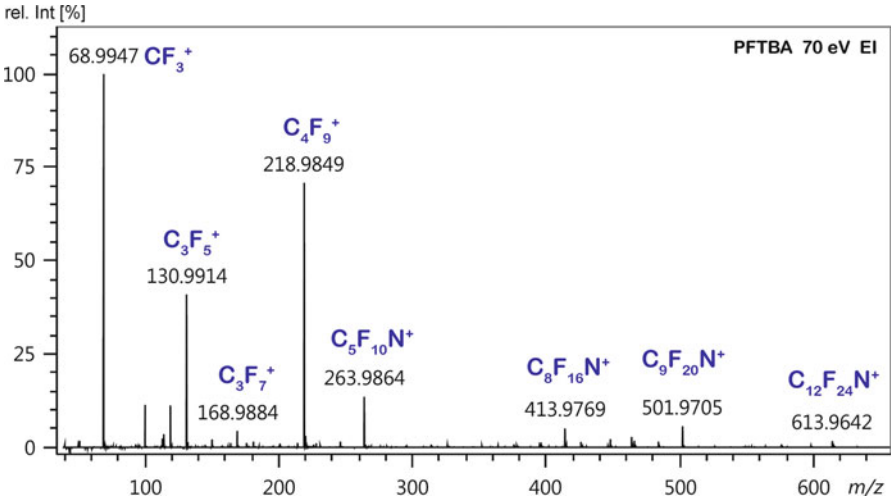

Fig. 3.30 EI mass spectrum of PFTBA with the composition of the most significant reference ions assigned. The calibration has already been performed, and thus, the *m*/*z* values are accurate

compound yields peaks up to *m*/*z* 614 [44, 60]. Like PFK, PFTBA is admitted via the reference inlet. The spectrum of PFTBA shows a reasonable number of peaks to be used for mass calibration (Fig. 3.30). How many of them are actually being used depends on the mass reference list. Also, the operator will normally check the automated assignment of reference peaks and may remove outliers. Such outliers are often due to overlap with background or sample peaks, e.g., in case of internal calibration (next paragraph). Their deletion can substantially improve the final calibration curve in that it reduces the average mass error of the calibration points, i.e., this measure reduces the standard deviation of the curve. While calibration curves can in principle be straight lines, actual instrument characteristics are often better approximated by using higher-order polynomials to fit the data. For example, based on the same spectrum of PFTBA a 3rd-order polynomial calibration yielded a gently bent curve (Fig. 3.31a). Among 19 assigned peaks, three outliers were identified and deleted. Repetition of the calibration using the corrected set of 16 peaks and a 4th-order polynomial (Fig. 3.31b) resulted in a notable reduction of average error.

3.6.2.1 Mass Accuracy Depends on Many Variables

Mass accuracy strongly depends on various parameters such as resolving power, scan rate, scanning method, signal-to-noise ratio of the peaks, peak shapes, overlap of isotopic peaks at same nominal mass, mass difference between adjacent reference peaks, calibration method etc. For instance, there is a marked effect of ion statistics on mass accuracy (Fig. 3.32). While peaks based on 10^3 to 10^5 ions yield results in a 1–5 ppm window, losses in accuracy occur due to Coulombic repulsion above 10^5 ions and due to poor ion statistics below 10^3 ions. Even though

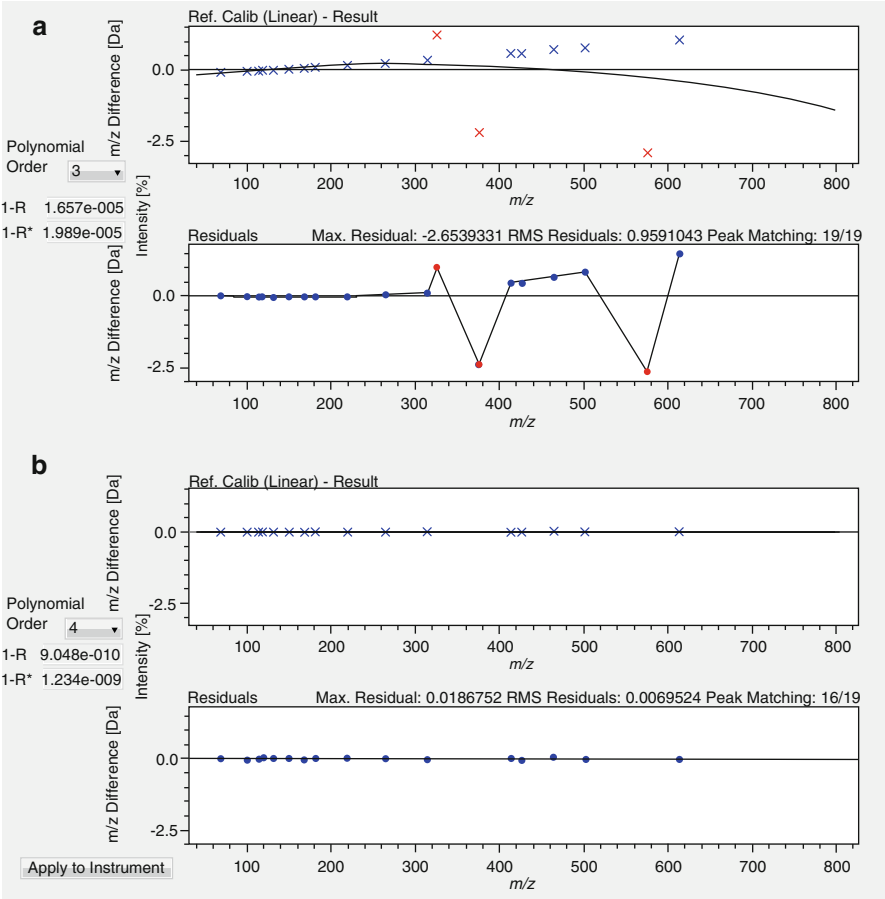

Fig. 3.31 Calibrations based on PFTBA. (**a**) 3rd-order polynomial calibration yields a gently bent curve. Three outliers (*red*) were identified and deleted. (**b**) Repetition of calibration using the corrected set of peaks and a 4th-order polynomial. Upon these measures, the correlation coefficients improve from the order of 10^{-5} to 10^{-9}. Figure composed of screenshots of JEOL AccuTOF GCx calibration software

determined for a specific Agilent GC-Q-TOF mass spectrometer, the basic characteristics of this graph can be assumed to be representative for most instruments.

It is also not possible to specify a general level of mass accuracy with external calibration. Depending on the type of mass analyzer and on the frequency of recalibration (monthly, weekly, daily, per sample), mass accuracy can vary from mediocre 0.5 u to perfect 10^{-3} u.

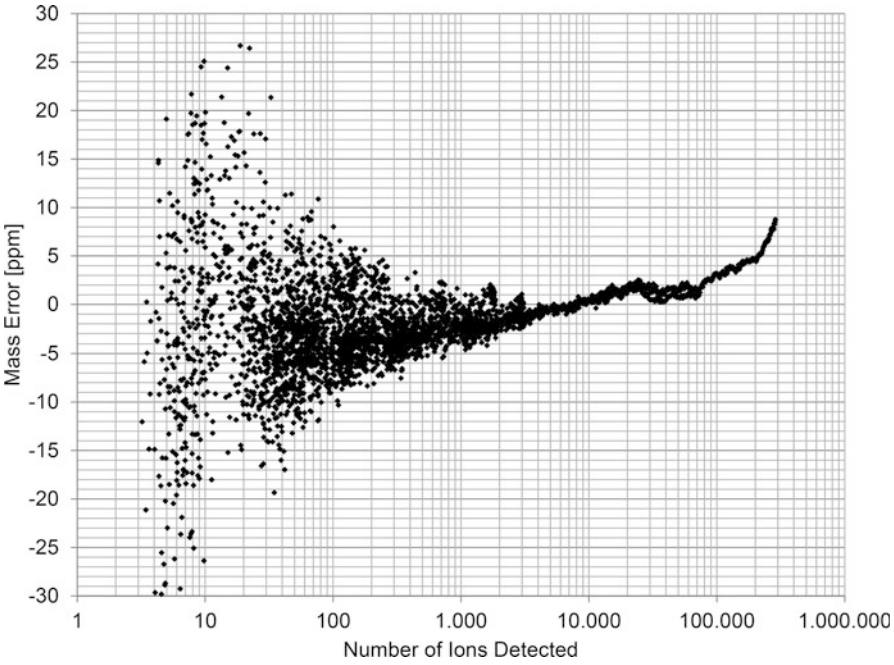

Fig. 3.32 Dependence of mass accuracy versus ion statistics as determined of a GC-Q-TOF instrument (Reproduced with kind permission of Bill Russ, Agilent Technologies)

3.6.3 Internal Mass Calibration

In principle, highest mass accuracy is achieved via *internal mass calibration*. The calibration compound can be introduced from a second inlet system or be mixed with the analyte prior to analysis. Mixing calibration compounds with the analyte requires some operational skills in order for it not to modify the analyte or to be modified itself. Therefore, a separate inlet for introducing the calibration compound is preferred. This can be done by introducing volatile standards such as PFK from a reference inlet system in electron ionization, by use of a dual-target probe in fast atom bombardment, or by use of a second sprayer in electrospray ionization. Internal mass calibration typically affords mass accuracies in the order of 0.1–0.5 ppm with FT-ICR, 0.5–1 ppm with Orbitrap, 0.5–5 ppm with magnetic sector, and 1–10 ppm with time-of-flight analyzers.

Overlap of PFK and sample For zirconium complexes the molecular ion range of an HR-EI spectrum is typified by the isotopic pattern of zirconium and chlorine (Fig. 3.33). ^{90}Zr represents the most abundant zirconium isotope which is accompanied by ^{91}Zr, ^{92}Zr, ^{94}Zr, and ^{96}Zr, all of them having considerable abundances. If the peak at *m*/*z* 414.9223 represents the monoisotopic ion, then the elemental composition containing ^{90}Zr and ^{35}Cl is the only correct interpretation. Thus, the formula $C_{16}H_{14}NCl_3Zr$ can be identified from the composition list (Fig. 3.34). Next, the X + 2 and X + 4 compositions should mainly be due to $^{35}Cl_2$

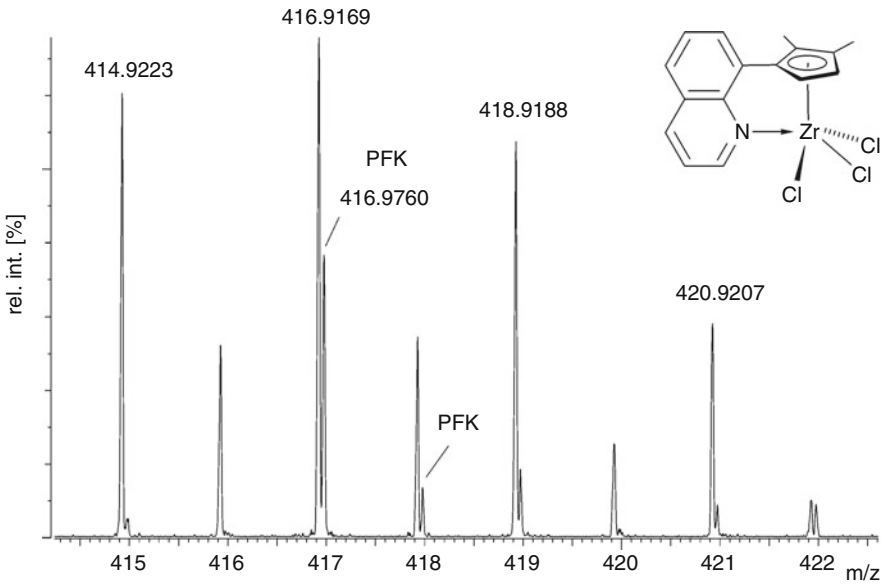

Fig. 3.33 Partial high-resolution EI mass spectrum in the molecular ion region of a zirconium complex. At $R = 8000$ the PFK ion can barely be separated from the slightly more mass-deficient analyte ion (By courtesy of M. Enders, Heidelberg University)

^{37}Cl and $^{35}Cl_{37}Cl_2$, respectively, leading to their identification. All formulas must have a remainder of $C_{16}H_{14}N$ in common. In this example, $R = 8000$ is the minimum to separate the PFK reference peak at m/z 417 from that of the analyte. Otherwise, the mass assignment would have been wrong because the peak at m/z 417 would then be centered at a weighted mass average of its two contributors. Alternatively, such a peak may be omitted from both reference list and composition list.

3.6.4 Specification of Mass Accuracy

Measured accurate masses, when used to assign molecular formulas, should always be accompanied by their mass accuracies [61]. Ideally, this can be done by giving the mean mass value and the corresponding error in terms of standard deviation through several repeated measurements of the same ion [44]. This is definitely not identical to the error usually provided with a mass spectrometer's software, where the error is based on the difference of a single pair of calculated and measured values. The reduction of the average mass error goes with the square root of the number of determinations (Sect. 3.5.4) [43].

Identifying the $[M\text{-}Cl]^+$ ion of chloroform The $[M\text{-}Cl]^+$ ion, $[CHCl_2]^+$, represents the base peak in the EI spectrum of chloroform. The results of three

```
Inlet : Direct                          Ion Mode : EI+
RT : 1.94 min                           Scan#: 5
Elements : C 40/0, H 40/0, N 2/0, Cl 3/0(35Cl 3/0, 37Cl 3/0), Zr 1/0
Mass Tolerance       : 5mmu
Unsaturation (U.S.) : 0.0 - 100.0

Observed m/z Int%   Err[ppm / mmu]    U.S.  Composition
  414.9223     7.5     -0.4 /  -0.2   22.5  C 23 H 2 N 2 35Cl 37Cl 2
                  ---> -3.9 /  -1.6   10.0  C 16 H 14 N 35Cl 3 Zr
                      -15.3 /  -6.3   15.0  C 19 H 11 N 35Cl 37Cl Zr
                       -0.8 /  -0.3   15.5  C 20 H 11 37Cl 2 Zr

  416.9169     8.9     -6.2 /  -2.6   22.5  C 23 H 2 N 2 37Cl 3
                       +3.1 /  +1.3   28.0  C 26 H N Zr
                  ---> -9.7 /  -4.0   10.0  C 16 H 14 N 35Cl 2 37Cl Zr
                       +9.1 /  +3.8   15.5  C 18 H 9 N 2 37Cl 2 Zr
                       +4.8 /  +2.0   10.5  C 17 H 14 35Cl 37Cl 2 Zr

  418.9188     7.5     -8.2 /  -3.4   24.5  C 26 H 2 35Cl 3
                       +0.2 /  +0.1   27.5  C 25 H N 2 Zr
                       -4.2 /  -1.7   22.5  C 24 H 6 35Cl Zr
                  ---> +1.8 /  +0.8   10.0  C 16 H 14 N 35Cl 37Cl 2 Zr
```

Fig. 3.34 Possible elemental compositions of the zirconium complex shown in the preceding figure. The error for each proposal is listed in units of ppm and "mmu" (0.001 u). U.S. = "unsaturation", i.e., the number of rings and/or double bonds (Sect. 6.4.4). For simplicity, here the correct assignments are highlighted with an *arrow* (By courtesy of M. Enders, Heidelberg University)

subsequent determinations for the major peaks of the isotopic pattern are listed below (Fig. 3.35). The typical printout of a mass spectrometer's data system provides experimental accurate mass and relative intensity of the signal along with absolute and relative mass error as calculated for a set of suggested formulas. Here, the experimentally accurate mass values yield a root-mean-square of 82.9442 ± 0.0006 u for the $[^{12}CH^{35}Cl_2]^+$ ion. The comparatively small standard deviation of 0.0006 u corresponds to a relative error of 7.5 ppm.

Balanced settings for best results

There is always a trade-off between resolving power, signal intensity, and mass accuracy. Mass accuracy may even suffer from overly ambitious settings of resolving power if this ends up in causing noisy peaks. Often, centroids are determined more accurately from smooth and symmetrically shaped peaks at somewhat lower resolving power. One should be aware of the fact that the position of a peak of 0.1 u width, for example, has to be determined to $^1/_{50}$ of its width to obtain 0.002 u accuracy [36].

```
[ Elemental Composition ]
Data  : JMS18120_009                    Date : 14-May-2002 08:20
Sample: CHCl3
Elements : C 10/1(12C 10/0, 13C 1/0), H 10/0, Cl 4/0(35Cl 4/0, 37Cl 4/0)
Mass Tolerance       : 10mmu
Unsaturation (U.S.) : -200.0 - 200.0

Observed m/z Int%   Err[ppm / mmu]    U.S.  Composition
   82.9433   100.0    +27.5 /  +2.3    1.0  13C 35Cl 2
                      -26.4 /  -2.2    0.5  12C H 35Cl 2

   84.9406    62.5    +29.5 /  +2.5    1.0  13C 35Cl 37Cl
                      -23.2 /  -2.0    0.5  12C H 35Cl 37Cl

   86.9379    10.1    +31.6 /  +2.7    1.0  13C 37Cl 2
                      -19.9 /  -1.7    0.5  12C H 37Cl 2

Observed m/z Int%   Err[ppm / mmu]    U.S.  Composition
   82.9449   100.0    +45.8 /  +3.8    1.0  13C 35Cl 2
                       -8.1 /  -0.7    0.5  12C H 35Cl 2

   84.9422    66.0    +48.0 /  +4.1    1.0  13C 35Cl 37Cl
                       -4.7 /  -0.4    0.5  12C H 35Cl 37Cl

   86.9404    11.2    +60.3 /  +5.2    1.0  13C 37Cl 2
                       +8.9 /  +0.8    0.5  12C H 37Cl 2

Observed m/z Int%   Err[ppm / mmu]    U.S.  Composition
   82.9447   100.0    +43.7 /  +3.6    1.0  13C 35Cl 2
                      -10.2 /  -0.8    0.5  12C H 35Cl 2

   84.9419    65.1    +44.6 /  +3.8    1.0  13C 35Cl 37Cl
                       -8.1 /  -0.7    0.5  12C H 35Cl 37Cl

   86.9391    10.8    +45.1 /  +3.9    1.0  13C 37Cl 2
                       -6.3 /  -0.6    0.5  12C H 37Cl 2
```

Fig. 3.35 Printout of elemental compositions of the $[M–Cl]^+$ ion of chloroform as obtained from three subsequent measurements (70 eV EI, $R = 8000$). The error for each proposal is listed in units of ppm and "mmu" (outdated for mu). U.S. ("unsaturation") is the number of rings and/or double bonds (Sect. 6.4.4)

3.6.5 Identification of Formulas from HR-MS Data

The experimentally determined accurate mass of an ion should lie within a reasonable error range independent of the ionization method and the instrument used [62]. The correct (expected) composition is not necessarily the one with the least error but just one within the experimental error interval. You should examine the examples in Figs. 3.34 and 3.35 to verify that the correct formulas can have a larger mass error than illogical ones.

Often, computer-generated formula lists contain suggested formulas that are not reasonable from a chemical point of view or are in contradiction to mass spectrometric rules. When searching for the correct formula of an ion you need to consider some basic rules:

- All elements that have to be taken into account have to be admitted in suitable numbers when the list is being created.
- Depending on the ionization method, even-electron or odd-electron ions may be formed. This criterion can rule out some compositions.
- Also, dependent on the ionization method, molecules may form $M^{+\bullet}$, $[M + H]^+$, $[M + NH_4]^+$, $[M + \text{alkali}]^+$ ions and others. Therefore, reasonable adducts have to be taken into account.
- The assigned formula must be in accordance with the experimentally observed and the calculated isotopic pattern for the assumed composition.
- The formula has to obey the nitrogen rule (Sect. 6.2.7)
- Formulas in contradiction to one of these points are erroneous.

The latest software packages for formula generation from accurate mass tend to imply such rules by offering selections not only on error interval, elements, and number thereof to be taken into account but also of odd-electron and/or even-electron species, ranges of H/C ratio, ranking by correlation to calculated isotopic pattern etc. [63]. Additionally, $\Delta(m/z)$ between isotopic peaks of the same element should be used as a source of information [64] (Sect. 3.7.2.1). Whatever the level of sophistication of such software tools, obtaining correct results still requires knowledgeable operator input and eventually refinement after communicating with the person who provided the sample.

Formula calculation for a silicone Silicone oligomers as present in silicone oil and rubber can readily be analyzed using direct analysis in real time (DART) mass spectrometry in positive-ion mode on a Fourier transform-ion cyclotron resonance (FT-ICR) instrument [65, 66]. Under these conditions, the silicone oligomers form ammonium adduct ions where the number of O atoms equals that of Si atoms. The signals also exhibit marked Si isotope patterns (Fig. 3.11). The example shows a screenshot of a formula calculation for a 13mer silicone ion with the monoisotopic ion at m/z 980.27736 (Fig. 3.36). The formula list is calculated within restrictive limits for elemental composition $C_{20–30}H_{60–90}O_{10–14}Si_{10–14}$, mass error of 5 ppm, and for even-electron ions only. Nonetheless, there is still a selection among ten candidates; a tighter error interval would have further reduced the number (Sect. 3.5.6). In this case, the assignment was assisted by the fact that the ion belongs to a homologous series. The correct composition, $[C_{26}H_{82}O_{13}Si_{13}]^+$, is highlighted by a blue bar [66].

3.7 Resolution Interacting with Isotopic Patterns

3.7.1 Multiple Isotopic Compositions at Very High Resolution

We started our lesson on isotopic patterns with the unspoken assumption of nominal mass resolution, which makes it much easier to understand how isotopic patterns are formed. The procedure of summing up all isotopic abundances contributing to

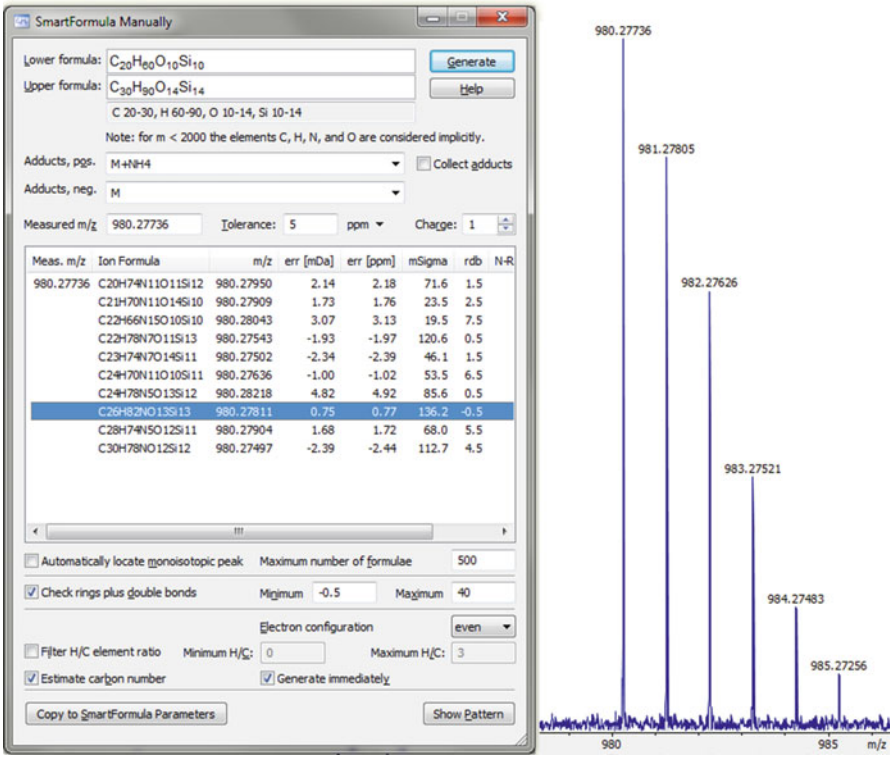

Fig. 3.36 Screenshot of formula calculation for a silicone ion using Bruker SmartFormula software (*left*) and the corresponding signal (*right*) as obtained by DART-FT-ICR-MS. The formula list is calculated within restrictive limits for elemental composition $C_{20–30}H_{60–90}O_{10–14}Si_{10–14}$, mass error of 5 ppm, and even-electron ions only. The correct composition of the NH_4^+ adduct ion, *m*/*z* 980.27736, is highlighted by a blue bar

the same nominal mass is correct as long as very high resolution is not employed. In that case, following such a simplified protocol is acceptable, because generally isobaric isotopolog ions are very similar in mass [25].

In the earlier introduction of resolution it should have become clear that very high resolution is capable of separating different isotopic compositions of the same nominal mass, thereby giving rise to multiple peaks on the same nominal *m*/*z* (Figs. 3.21, 3.22, and 3.32). In molecules with masses of around 10,000 u, a single unresolved isotopic peak may consist of as many as 20 different isotopic compositions (also cf. Fig. 3.39) [67, 68].

Imagine infinite resolution Numerous isotopologs contribute to the isotopic pattern of $C_{16}H_{20}OSi$. Among them the monoisotopic ion at *m*/*z* 256.1283 is the most abundant (Fig. 3.37). For the first isotopic peak at *m*/*z* 257 the major contribution derives from ^{13}C, but ^{29}Si and ^{17}O also play a role. Actually, ^{2}H should also be

m/z	composition	rel. int. [%]	
256.12836	C16.H20.O.Si	100.00000	monoisotopic
257.12790	C16.H20.O.29Si	5.10957	1st isotopic
257.13171	C15.13C.H20.O.Si	17.92663	
257.13257	C16.H20.17O.Si	0.03709	
258.12518	C16.H20.O.30Si	3.38468	2nd isotopic
258.13126	C15.13C.H20.O.29Si	0.91597	
258.13214	C16.H20.17O.29Si	0.00190	
258.13260	C16.H20.18O.Si	0.20449	
258.13507	C14.13C2.H20.O.Si	1.50639	
258.13593	C15.13C.H20.17O.Si	0.00665	
259.12854	C15.13C.H20.O.30Si	0.60676	3rd isotopic
259.12939	C16.H20.17O.30Si	0.00126	
259.13214	C16.H20.18O.29Si	0.01045	
259.13461	C14.13C2.H20.O.29Si	0.07697	
259.13550	C15.13C.H20.17O.29Si	0.00034	
259.13596	C15.13C.H20.18O.Si	0.03666	
259.13843	C13.13C3.H20.O.Si	0.07876	
259.13928	C14.13C2.H20.17O.Si	0.00056	
260.12943	C16.H20.18O.30Si	0.00692	4th isotopic
260.13190	C14.13C2.H20.O.30Si	0.05099	
260.13275	C15.13C.H20.17O.30Si	0.00023	
260.13550	C15.13C.H20.18O.29Si	0.00187	
260.13797	C13.13C3.H20.O.29Si	0.00402	
260.13885	C14.13C2.H20.17O.29Si	0.00003	
260.13931	C14.13C2.H20.18O.Si	0.00308	
260.14175	C12.13C4.H20.O.Si	0.00287	
260.14264	C13.13C3.H20.17O.Si	0.00003	

Fig. 3.37 Tabular representation of the theoretical isotopic distribution of $C_{16}H_{20}OSi$ at infinite resolution. The contribution of ^{2}H is not considered, and isotopic peaks above *m*/*z* 260 are omitted due to their minor intensities

considered, but has been omitted due to its extremely low isotopic abundance. As the isotopologs of the same nominal *m*/*z* are not true isobars, their intensities will not sum up in one common peak. Instead, they are detected side by side provided sufficient resolving power is available. The pair $^{13}C^{12}C_{15}H_{20}{}^{16}OSi$, *m*/*z* 257.13171, and $^{12}C_{16}H_{20}{}^{17}OSi$, *m*/*z* 257.13257, roughly necessitates 3×10^5 resolution ($R = 257/0.00086 = 299{,}000$). There are six different compositions contributing to the second isotopic peak at *m*/*z* 258 and even eight for the third isotopic peak at *m*/*z* 259. Again, it is the merit of FT-ICR-MS that resolutions in the order of several 10^5 are now available although *ultrahigh resolution*, as this is termed, is still not fully routine on those instruments (Sect. 4.7).

Telling $^{13}C_2$ and ^{34}S peaks apart Peptides often contain sulfur from cysteine. Provided there are at least two cysteines in the peptide molecule, sulfur can be in the form of thiol group (SH, reduced) or sulfur bridges (S–S, oxidized). Often, both forms are contained in the same sample. At ultrahigh resolution, the contributions

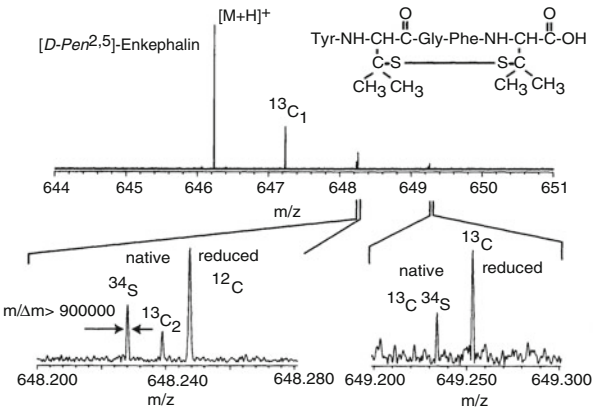

Fig. 3.38 [D-Pen^{2,5}] Enkephalin – Ultrahigh-resolution MALDI-FT-ICR mass spectrum of native (S–S) and reduced (2 × SH) forms. The expanded *m/z* views of the second and third isotopic peak show fully mass-resolved signals (Reproduced from Ref. [69] with permission. © American Chemical Society, 1997)

of these compositions to the same nominal *m/z* can be distinguished. The ultrahigh-resolution matrix-assisted laser desorption/ionization (MALDI) FT-ICR mass spectrum of native and reduced [D-Pen^{2,5}]enkephalin is an example of such a separation (Fig. 3.38) [69]. The left expanded view shows fully resolved peaks due to ^{34}S and $^{13}C_2$ isotopologs of the native and the all-^{12}C peak of the reduced compound at *m/z* 648. The right expansion reveals the $^{13}C_1{}^{34}S$ peak of the native plus the $^{13}C_1$ signal of the reduced form at *m/z* 649. Here, R_{FWHM} is more than 9×10^5.

3.7.2 Isotopologs and Accurate Mass

It has been pointed out that routine accurate mass measurements are conducted at resolutions which are normally too low to separate isobaric isotopologs. Unfortunately, multiple isotopic compositions under the same signal tend to distort the peak shape (Fig. 3.39) [68]. This effect causes problems when elemental compositions have to be determined from such multi-isotopolog peaks, e.g., if the mono- isotopic peak is too weak as in case of many transition metals. Generally, the observed decrease in mass accuracy is not dramatic and is somewhat counterbalanced by the information derived from the isotopic pattern. However, it can be observed that mass accuracy decreases by about 50% on such unresolved signals.

3.7.2.1 Information from Accurate Mass Differences Between Isotopes

If isotopolog ions are resolved or if certain isotopologs are free from interference, and provided sufficient mass accuracy is available, $\Delta(m/z)$ between isotopic peaks can yield adequate analytical information [64]. As are the isotopic masses themselves, the differences between isotopic masses are characteristic for certain elements. Boron for example, has a small mass difference of just 0.9964 u between ^{10}B and ^{11}B, whereas the pair of ^{191}Ir and ^{193}Ir presents a rare example of a difference clearly above 2 u, which is still distinguishable from hydrogenation. Determination of $\Delta(m/z)$ values can thus help to distinguish between hydrogenation

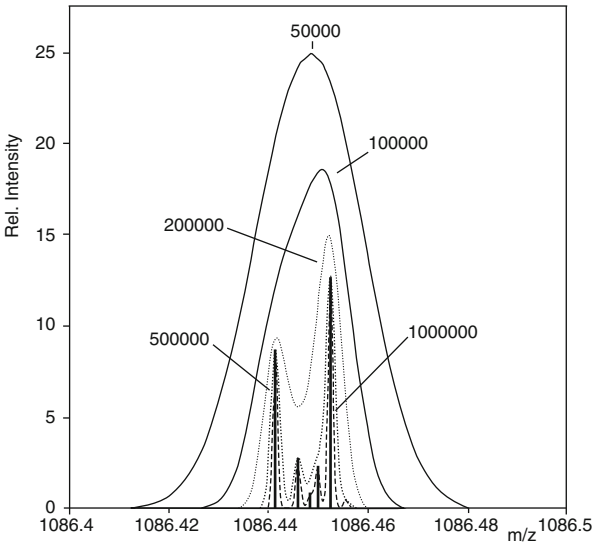

Fig. 3.39 Arg^8 vasopressin – Theoretical effect of resolution on the shape of the M + 2 peak at *m/z* 1086.4. Theoretical mass spectra of the $[vasopressin + H]^+$ ion and the five indicated resolution values (FWHM) have been superimposed and the bar spectrum corresponds to infinite resolution (Adapted from Ref. [68] with permission. © John Wiley and Sons Ltd., 1994)

and X + 2 element isotopic peaks can ascertain the presence of boron vs. loss of a hydrogen radical etc. Some helpful values are compiled in Table 3.3. Obviously, there are also limits to this approach, for example, when a decision between M + 2 due to ^{37}Cl or ^{65}Cu is called for, in particular, as their isotopic abundances are also similar.

Isotopic pattern of substance P at R = 4 million Werlen (Fig. 3.39) [68] had anticipated that ultrahigh resolution would reveal multiple peaks. Modern FT-ICR instruments are, in fact, able to resolve these peaks [70, 71]. The peaks contributing to the isotopic pattern of doubly protonated substance P, a peptide ion of the composition $[C_{63}H_{100}O_{13}N_{18}S]^{2+}$, have been measured one by one at R = 4,000,000. (To avoid space charge effects and to operate at optimum ion population – a limitation inherent to FT-ICR-MS – the ultimate resolving power was achieved via the measurement of isolated isotopologs.)

The set of four partial spectra in Fig. 3.40 reflects the increasing complexity of the isotopic composition as one moves from [M + 1] (Fig. 3.40a) to [M + 4] (Fig. 3.40d). The most relevant contributions to the [M + 4] ion in order of rising mass are formed by combinations of $^{13}C^{15}N^{34}S$, $^{34}S^{18}O$, $^{13}C_2{}^{34}S$, $^{13}C^{15}N^{18}O$, $^{13}C_3{}^{15}N$, $^{13}C_3{}^{33}S$, $^{13}C_2{}^{18}O$, and finally $^{13}C_4$. The masses of these ions spread across just 8.63 mu between the lightest and the heaviest of the group. Note that the pure $^{13}C_X$ isotopic ion is always that of highest *m/z* within the respective [M + X] ion provided that only C, H, N, O, and S are involved (some peaks of very low intensity may occur above).

Ultrahigh resolving power alone is merely able to separate the various isotopic contributions belonging to [M + 1] to [M + 4] ions. Key to the assignment of these compositions is the knowledge of the accurate mass differences between certain

Table 3.3 Characteristic mass differences to identify the presence of elements

Pair of isotopes or modification	Δm [u]
^{6}Li vs. ^{7}Li	1.0009
^{10}B vs. ^{11}B	0.9964
^{12}C vs. ^{13}C	1.0033
^{32}S vs. ^{34}S	1.9958
^{35}Cl vs. ^{37}Cl	1.9970
^{58}Ni vs. ^{60}Ni	1.9955
^{63}Cu vs. ^{65}Cu	1.9982
^{79}Br vs. ^{81}Br	1.9980
^{191}Ir vs. ^{193}Ir	2.0023
gain or loss of H	1.0078
gain or loss of H_2	2.0156

pairs of isotopologs (Table 3.3). The $^{13}C_X$ peak, for example, will be located at $m/z_{\text{monoisotopic}} + 1.0033 \times X$ (note that $\Delta m/z$ is half of the mass difference in case of a doubly charged ion as $z = 2$, Sect. 3.8). Thus, assignment of isotopic peaks is achieved by their accurate mass differences. Vice versa, the reliability of the assignment of elemental compositions increases the better the suggested formula complies with the measured isotopic fine structure; modern data analysis software packages exploit this to their advantage.

3.7.3 Large Molecules – Isotopic Patterns at Sufficient Resolution

Terms such as *large molecules* or *high mass* are subject to steady change in mass spectrometry as new techniques for analyzing high-mass ions are being developed or improved [72]. Here, the focus is on masses in the range of 10^3–10^4 u.

With increasing m/z the center of the isotopic pattern, i.e., the *average molecular mass*, is shifted to values higher than the *monoisotopic mass*. The center, i.e., the average mass, may not be represented by a real peak, but it tends to be close to the peak of *most abundant* mass (Fig. 3.41). The monoisotopic mass is of course still related to a real signal, but it may be of such a low intensity that it is difficult to recognize. Finally, the *nominal mass* becomes a mere number which is no longer useful to describe the molecular weight [41, 67].

The calculation of isotopic patterns of molecules of several 10^3 u is not a trivial task, because slight variations in the relative abundances of the isotopes encountered gain relevance and may shift the most abundant mass and the average mass up or down by 1 u. In a similar fashion the algorithm and the number of iterations employed to perform the actual calculation affect the final result [25].

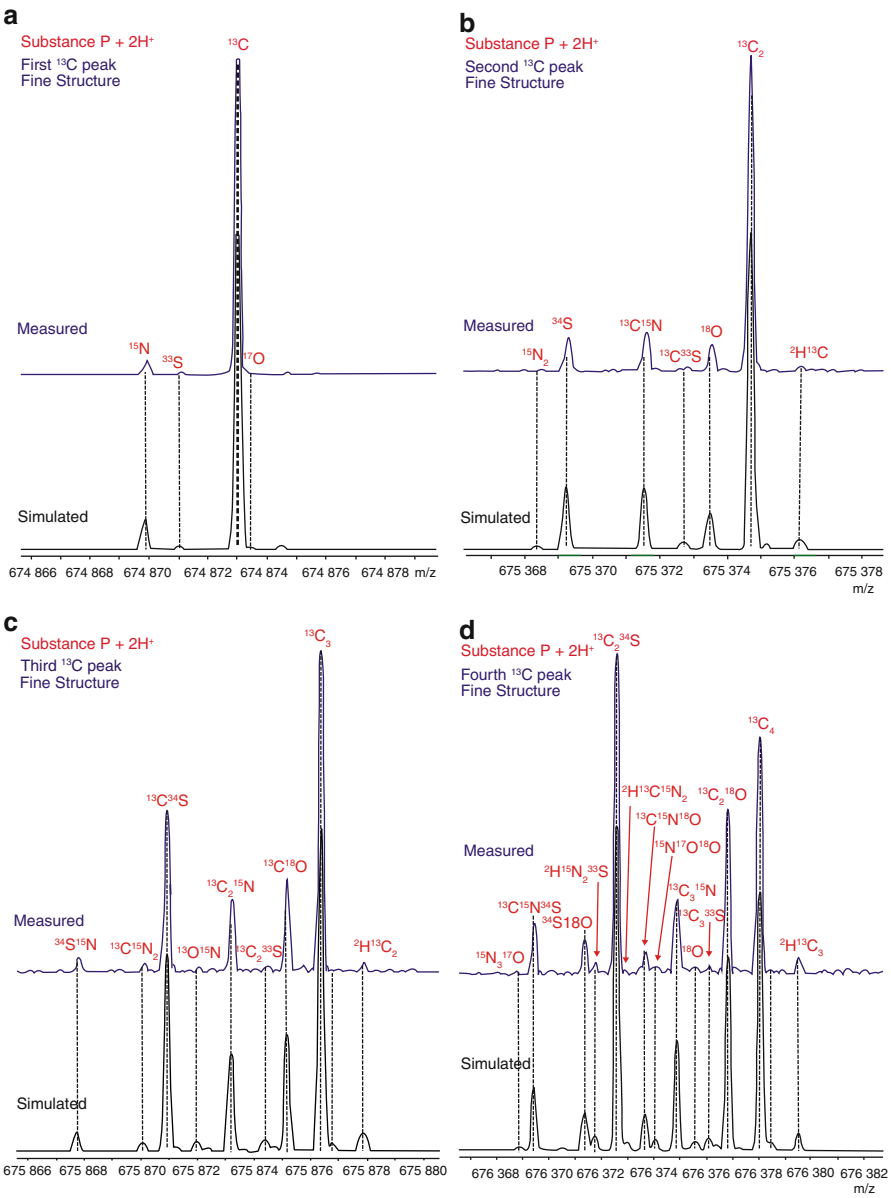

Fig. 3.40 Isotope peaks of doubly protonated substance P, $[C_{63}H_{100}O_{13}N_{18}S]^{2+}$, as measured individually by FT-ICR-MS at $R = 4{,}000{,}000$. (**a**) First isotopic peak, [M + 1], (**b**) [M + 2], (**c**) [M + 3], and (**d**) [M + 4]. The most relevant contributions are due to ^{13}C, ^{34}S, and ^{18}O. The [M + 4] signal splits into eight major and several very minor peaks (Reproduced from Ref. [70] by permission. © American Chemical Society, 2012)

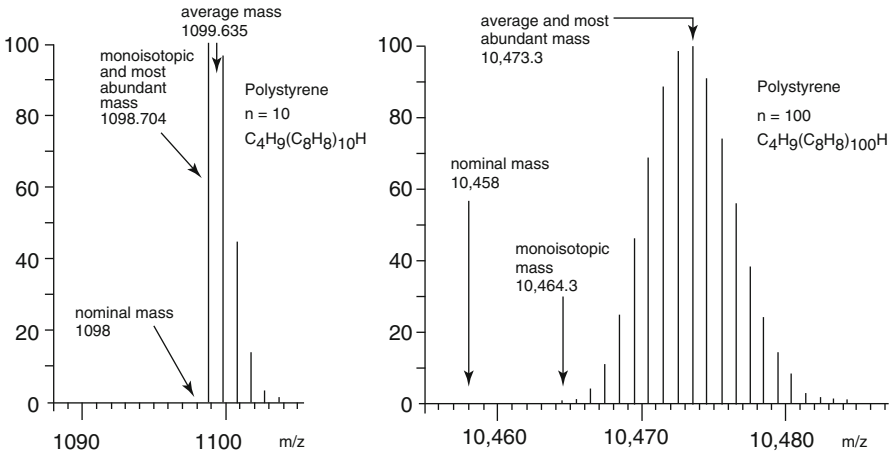

Fig. 3.41 Polystyrene. Calculated isotopic patterns of large ions (Adapted from Ref. [67] with permission. © American Chemical Society, 1983)

Mass of large molecules

The calculation of relative molecular mass, M_r, of organic molecules exceeding 2000 u is significantly influenced by the basis it is performed on. Both the atomic weights of the constituent elements and the natural variations in isotopic abundance contribute to the differences between *monoisotopic*- and *relative atomic mass-based* M_r values. In addition, they tend to characteristically differ between major classes of biomolecules. This is primarily because of molar carbon content, e.g., the difference between polypeptides and nucleic acids is about 4 u at $M_r = 25{,}000$ u. Considering terrestrial sources alone, variations in the isotopic abundance of carbon lead to differences of about 10–25 ppm in M_r which is significant with respect to mass measurement accuracy in the region up to several 10^3 u [41].

3.7.4 Isotopic Patterns of Macromolecules Versus Resolution

It is certainly desirable to have at least sufficient resolution to resolve isotopic patterns to their nominal mass contributions. However, not every mass analyzer is capable of doing so with any ion it can pass through. Such conditions often occur when ions of several thousand u are being analyzed by quadrupole, time-of-flight or quadrupole ion trap analyzers, and hence it is useful to know about the changes in spectral appearance and their effect on peak width and detected mass [68].

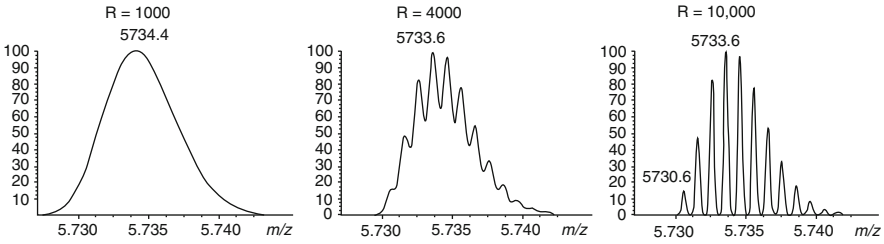

Fig. 3.42 Bovine insulin – the isotopic pattern calculated for $[M + H]^+$ at different resolutions ($R_{10\%}$). Note that the envelope at $R = 1000$ is wider than the real isotopic pattern

Isotopic pattern of bovine insulin The isotopic pattern of the $[M + H]^+$ ion of bovine insulin, $[C_{254}H_{378}N_{65}O_{75}S_6]^+$, has been calculated for $R_{10\%} = 1000$, 4000, and 10,000. At $R = 1000$ the isotopic peaks are not resolved (Fig. 3.42) and an envelope smoothly covering the isotopic peaks is observed instead; it is even slightly wider than the real isotopic pattern. The maximum of this envelope is in good agreement with the calculated average mass, i.e., the molecular weight (Eq. 3.2). At $R = 4000$ the isotopic peaks become sufficiently resolved to be recognized as such. The m/z values are very close to the corresponding isotopic masses; however, there can be some minor shifts due to their still significant overlap. Finally, at $R = 10{,}000$ the isotopic pattern is well resolved and interferences between isotopic peaks are avoided. The next step, i.e., to resolve the multiple isotopic contributions to each of the peaks would require $R > 10^6$.

Fading separation at high *m/z* Dendrimers are a class of synthetic macromolecules that can be synthesized at various sizes. A special set of monodisperse dendrimers has thus been developed for mass calibration in MALDI-MS, in particular with time-of-flight (TOF) analyzers in mind [73]. Depending on the actual MALDI-TOF instrument some of the higher m/z dendrimers are at or just beyond the limits of resolving power, i.e., the isotopic separation is fading away as one moves along the series of peaks. The positive-ion MALDI-TOF spectrum of such a SpheriCal mixture ($C_{398}H_{468}O_{138}$, $C_{529}H_{620}O_{184}$, $C_{660}H_{772}O_{230}$, $C_{796}H_{934}O_{277}$) exemplifies this behavior upon transition from about m/z 7600 to 15,000 (Fig. 3.43) [74].

3.8 Charge State and Interaction with Isotopic Patterns

Even though singly charged ions seem to be the dominant species in mass spectrometry at first sight, there are many applications where doubly and multiply charged ions are of utmost importance. In electrospray ionization (Chap. 12) even extremely high *charge states* can be observed, e.g., up to 60-fold in case of proteins of about 60,000 u molecular weight. Doubly and triply charged ions are also common in electron ionization (Chaps. 5 and 6) and field desorption (Chap. 8).

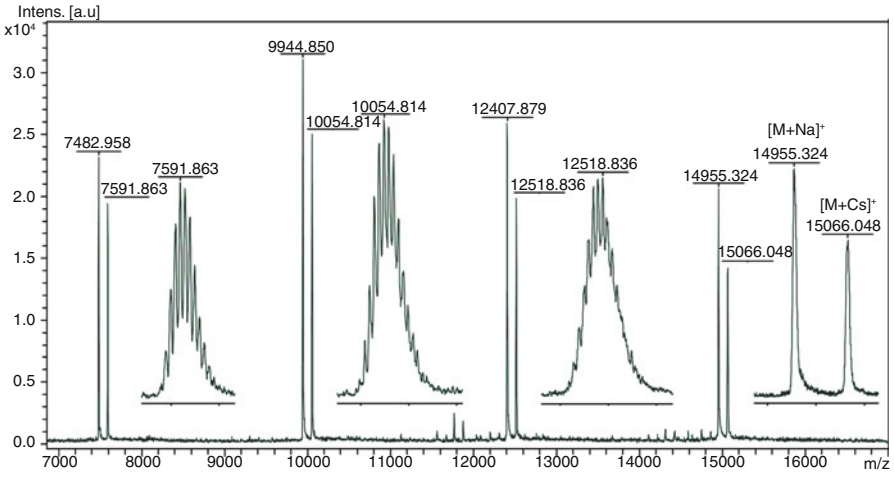

Fig. 3.43 Positive-ion MALDI-TOF spectrum of a SpheriCal kit (PFS-14) as obtained in the presence of Na^+ and Cs^+ ions where each of the four dendrimers forms $[M + Na]^+$ and $[M + Cs]^+$ ions leading to eight reference peaks in total. The insets show expanded views of the isotopic patterns of the respective $[M + Cs]^+$ ion signals. As m/z increases, resolution of isotopic peaks can no longer be achieved (Adapted from Ref. [74] with permission. © Springer-Verlag, Heidelberg, 2016)

The effect of higher charge states are worth considering. As z increases from 1 to 2, 3 etc., the numerical value of m/z is reduced by a factor of 2, 3 etc., i.e., the ion will be detected at lower m/z than the corresponding singly charged ion of the same mass. In general, the entire m/z scale is compressed by a factor of z if $z > 1$.

Consequently, the isotopic peaks are then located at $\Delta(m/z) = {}^1/_z$. Vice versa, the charge state is obtained from the reciprocal value of the distance between adjacent peaks, e.g., peaks at $\Delta m/z = {}^1/_3$ correspond to $z = 3$, i.e., triply charged ions. The reasons for the compression of the m/z scale are discussed later (Sect. 4.2).

Isotopic patterns of $M^{+\bullet}$, M^{2+}, and $M^{3+\bullet}$ The EI mass spectrum of C_{60} also shows an abundant doubly charged molecular ion, ${C_{60}}^{2+}$, at m/z 360 with its isotopic peaks located at $\Delta(m/z) = 0.5$ and a ${C_{60}}^{3+\bullet}$ signal at m/z 240 of very low intensity (Fig. 3.44) [32]. The isotopic pattern remains unaffected by the charge state. As a consequence of the compressed m/z scale, the doubly charged ${C_{58}}^{2+}$ fragment ion is detected at m/z 348.

Isotopic distribution and charge state

Isotopic distributions are of course not affected by the charge state of an ion. Therefore, the relative intensities of the isotopic peaks are independent of the charge state. However, $\Delta m/z$ between the isotopic peaks is reduced by ${}^1/_z$,

(continued)

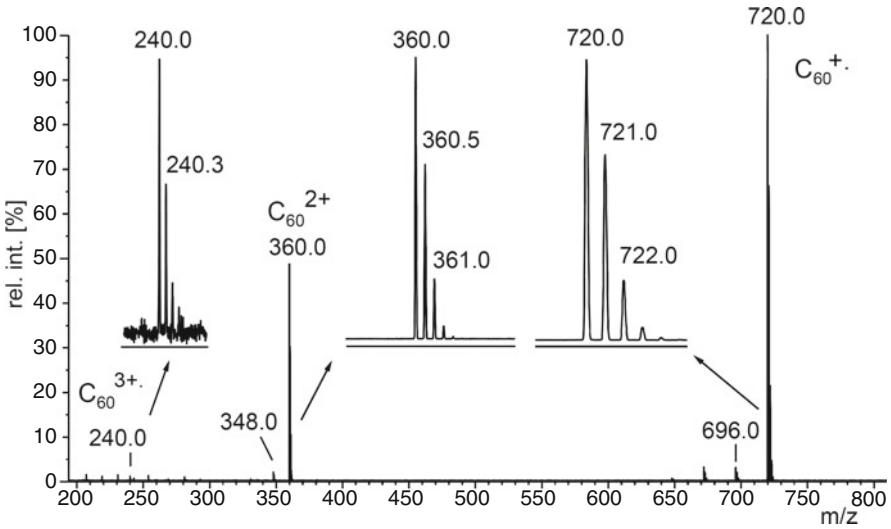

Fig. 3.44 EI mass spectrum of [60]Fullerene. The insets show the expanded signals of $M^{+\bullet}$, M^{2+}, and $M^{3+\bullet}$ ions. The signals of the patterns are at $\Delta m/z = 1$, 0.5, and 0.33, respectively. The intensity scale has been normalized in the insets to allow for easier comparison of the isotopic patterns (By courtesy of W. Krätschmer, Max Planck Institute for Nuclear Physics, Heidelberg)

thus allowing multiply charged ions to be easily distinguished from singly charged ions. Furthermore, the charge state can be directly determined from the reciprocal value of $^1/_z$.

3.9 Approaches to Visualize Complex HR-MS Data Sets

3.9.1 Deltamass

The term *deltamass* has been coined to define the mass value following the decimal point [75] thereby elegantly circumventing the somewhat unfortunate terminology related to the mass defect. The deltamass concept is only valid in the context for which it has been developed, i.e., to describe mass deviations of peptides from average values. Beyond this context, ambiguities arise from its rigorous application because *i*) a mass defect would then be expressed the same way as larger values of negative mass defect, e.g., in case of $^{127}I^+$ as 0.9045 u and in case of $C_{54}H_{110}{}^{+\bullet}$ as 0.8608 u, respectively, and *ii*) deviations of more than 1 u would be expressed by the same numerical value as those of less than 1 u.

Peptide modifications by deltamass The magnitude of mass defect can provide an idea of what compound class is being analyzed (Sect. 3.5.2). At a sufficient level of sophistication, mass defect can even reveal more detail [47]. Peptides consist of amino acids and therefore, their elemental compositions are rather similar independent of their size or sequence. This results in a characteristic relationship of formulas and deltamass values. Phosphorylation and more pronounced glycosylation cause lower deltamass, because they introduce mass-deficient atoms (P, O) into the molecule. The large number of hydrogens associated with lipidation, on the other side, contributes to a deltamass above normal level. On the average, an unmodified peptide of 1968 u, for example, shows a deltamass of 0.99 u, whereas a glycosylated peptide of the same nominal mass will have a value of 0.76 u. Therefore, the deltamass can be employed to obtain information on the type of covalent protein modification [75].

3.9.2 Kendrick Mass Scale

The intention of the *Kendrick mass scale* is to provide data reduction in a way that homologs can be recognized by their identical *Kendrick mass defect* (KMD). Due to the steadily increasing resolution and mass accuracy of modern instrumentation this issue is again gaining importance for complex mixture analysis by MS. The Kendrick mass scale is based on the definition $M_{(CH2)} = 14.0000$ u [76]. The conversion factor from the IUPAC mass scale, m_{IUPAC}, to the Kendrick mass scale, m_{Kendrick}, is therefore 14.000000/14.015650 = 0.9988834:

$$m_{\mathrm{Kendrick}} = 0.9988834\, m_{\mathrm{IUPAC}} \tag{3.15}$$

Next, we define the *Kendrick mass defect*, $m_{\mathrm{defectKendrick}}$, as

$$m_{\mathrm{defectKendrick}} = m_{\mathrm{nomKendrick}} - m_{\mathrm{Kendrick}} = \mathrm{KMD} \tag{3.16}$$

where $m_{\mathrm{nomKendrick}}$ is the *nominal Kendrick mass*, the closest integer to Kendrick mass.

Kendrick mass of $[C_{30}H_{49}O_3]^-$ The IUPAC mass of $[C_{30}H_{49}O_3]^-$ is 457.3687 u. The Kendrick mass of this ion is calculated as 457.3687 u × 0.9988834 = 456.8580 u. From this it follows that $m_{\mathrm{nomKendrick}} = 457$ u. The Kendrick mass defect of this ion is thus obtained as $m_{\mathrm{defectKendrick}} = 457$ u – 456.8580 u = 0.1419 u.

To translate spectral data into a useful *Kendrick mass plot*, a high-resolution mass spectrum is broken into segments of 1 u, which are aligned on the abscissa. Then, the Kendrick mass defect of the isobaric ions contained in the respective segment is plotted onto the ordinate. The resulting graph preserves not only the "coarse" spacing, e.g., about 1 u between odd and even mass values, but also the "fine structure", i.e., different Kendrick mass defects (KMDs) for different

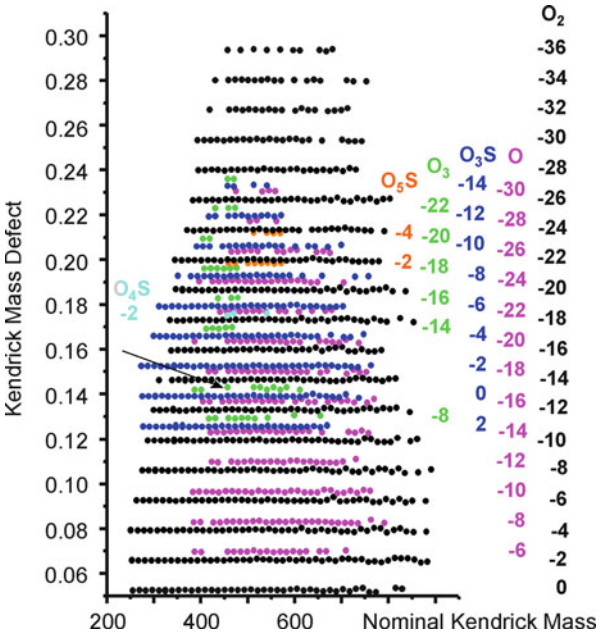

Fig. 3.45 Kendrick mass defect vs. nominal Kendrick mass for odd-mass $^{12}C_x$ ions ($[M–H]^-$ ions). The compound classes (O, O_2, O_3S, and O_4S) and the different numbers of rings plus double bonds (Sect. 6.4.4) are separated vertically. Horizontally, the points are spaced by CH_2 groups along a homologous series [77] (By courtesy of A.G. Marshall, NHFL, Tallahassee)

elemental compositions across each segment. Homologs are now easily recognized as horizontal rows in the plot [77].

Kendrick plots are becoming increasingly important as more instruments are able to provide ultrahigh resolution spectra of complex mixtures, and thus, create a demand for tools to retrieve analytically useful information from such large data sets [78–80]. Recently, Kendrick plots have been introduced as a tool for the convenient visualization of tandem mass spectral data of synthetic polymers, e.g., by referring to the monomeric building block as the base unit upon which the Kendrick mass defect is calculated [81].

Crude oil and diesel fuel In a Kendrick plot the composition of complex systems can be conveniently displayed. Several thousand elemental compositions in the ultrahigh resolution spectrum of petroleum crude oil [77] or diesel fuel [82] may be resolved. Such samples consist of numerous compound classes and/or alkylation series with some 30 homologs each that can be visually identified (Fig. 3.45). The formula employed for the preceding example is marked in the plot by an arrow.

3.9.3 Van Krevelen Diagrams

There is yet another tool for the display of composition characteristics of complex mixtures, the *van Krevelen diagram* [83]. The van Krevelen diagram is a plot of the atomic H/C ratio against the atomic O/C ratio. This plot causes the products related

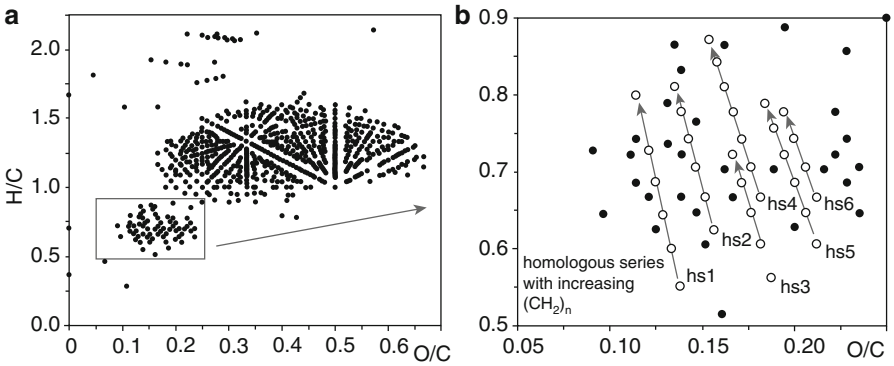

Fig. 3.46 Van Krevelen diagrams of deep-sea DOM. (**a**) Presentation of all molecules in 3500 m and 4600 m water depth. (**b**) Enlarged region of condensed polyaromatics where the members of the homologous series $(CH_2)_n$ with $n \geq 4$ are shown as *white circles* and connected along a *gray line* (Reproduced from Ref. [87] with permission. © Elsevier Science Publishers, 2006)

by reactions such as decarboxylation, dehydration, dehydrogenation, or oxidation to be displayed along straight lines. Along with KMD plots, the van Krevelen plot is therefore a major tool for the assessment of complex organic mixtures such as crude oil and its refinery products or the wide field of *natural organic matter* (NOM) that represents the largest share of biomass on earth [84–88].

Dissolved organic matter (DOM) The van Krevelen diagrams of HR-MS data obtained of deep-sea *dissolved organic matter* (DOM) show a group of molecules having low H/C (<0.9) and low O/C (<0.25) ratios clearly separated from each other (Fig. 3.46) [87]. An enlarged view of this group shows that it comprises 224 different molecular formulas corresponding to molecules that contain up to 35 rings and/or double bonds (r + d, Sect. 6.4.4). Homologous series can be identified along straight lines. Still this does not tell the complete structure of those molecules, but it delivers much more insight into the composition of DOM than pure accurate mass data alone.

3.10 Vantage Point on the World of Isotopes and Masses

Isotopes
Atoms belonging to the same element but different in mass due to a different number of neutrons in their nuclei are termed isotopes. Most elements occur naturally in two or three isotopes, others are monoisotopic and many are polyisotopic.

Isotopic Patterns
Mass spectrometry resolves matter by mass, and thus, separates atoms and molecules of different isotopic composition due to their difference in mass.

Consequently, the isotopic distribution is reflected by a mass spectrum as a set of peaks at neighboring m/z values.

Resolution
Separation of peaks relies on the ability of a mass spectrometer to resolve the signals corresponding to individual masses by virtue of its resolving power. Higher resolution provides additional information as species close in m/z can be separated in the spectrum. High resolution also results in more narrow peaks that can potentially be located more accurately on the m/z scale.

Accurate Mass
Accurate mass enables the assignment of molecular formulas due to the individual exact isotopic masses and the resulting distinguished masses of ions of given elemental composition. Besides sufficient resolving power to deliver sharp peaks, accurate mass measurements require careful mass calibration. Mass calibration can either be performed externally, i.e., prior to the analytical measurement, or internally by simultaneous admission of analyte and reference.

Ultrahigh Resolving Power
At ultrahigh resolving power, isotopic fine structure is resolved and different isotopic compositions of equal nominal mass, i.e., isotopolog ions, become separated. In addition, isobaric ions of different molecular formulas as present in complex mixtures become separated. Ultrahigh resolving power is therefore useful, or even a prerequisite, to analyze complex mixtures by MS.

Global Relevance of Mass Spectrometry
Understanding isotopic compositions of the elements, the way they are causing isotopic distributions and how they become expressed as isotopic patterns in mass spectra is absolutely essential for any use of mass spectral data. This also applies to accurate masses and the process of their translation into molecular formulas.

References

1. de Laeter JR, De Bièvre P, Peiser HS (1992) Isotope Mass Spectrometry in Metrology. Mass Spectrom Rev 11:193–245. doi:10.1002/mas.1280110303
2. Audi G (2006) The History of Nuclidic Masses and of Their Evaluation. Int J Mass Spectrom 251:85–94. doi:10.1016/j.ijms.2006.01.048
3. Budzikiewicz H, Grigsby RD (2006) Mass Spectrometry and Isotopes: A Century of Research and Discussion. Mass Spectrom Rev 25:146–157. doi:10.1002/mas.20061
4. Todd JFJ (1995) Recommendations for Nomenclature and Symbolism for Mass Spectroscopy Including an Appendix of Terms Used in Vacuum Technology. Int J Mass Spectrom Ion Proc 142:211–240. doi:10.1016/0168-1176(95)93811-F
5. McLafferty FW, Turecek F (1993) Interpretation of Mass Spectra. University Science Books, Mill Valley
6. Sparkman OD (2006) Mass Spectrometry Desk Reference. Global View Publishing, Pittsburgh
7. IUPAC (1998) Isotopic Composition of the Elements 1997. Pure Appl Chem 70:217–235

8. IUPAC, Coplen TP (2001) Atomic Weights of the Elements 1999. Pure Appl Chem 73:667–683
9. Price P (1991) Standard Definitions of Terms Relating to Mass Spectrometry. A Report From the Committee on Measurements and Standards of the Amercian Society for Mass Spectrometry. J Am Soc Mass Spectrom 2:336–348. doi:10.1016/1044-0305(91)80025-3
10. Busch KL (2001) Units in Mass Spectrometry. Spectroscopy 16:28–31
11. Platzner IT (1997) Applications of isotope ratio mass spectrometry. In: Modern Isotope Ratio Mass Spectrometry. Wiley, Chichester
12. Ferrer I, Thurman EM (2005) Measuring the Mass of an Electron by LC/TOF-MS: A Study of "Twin Ions". Anal Chem 77:3394–3400. doi:10.1021/ac0485942
13. Ferrer I, Thurman EM (2007) Importance of the Electron Mass in the Calculations of Exact Mass by Time-of-Flight Mass Spectrometry. Rapid Commun Mass Spectrom 21:2538–2539. doi:10.1002/rcm.3102
14. Schmidt HL (1986) Food Quality Control and Studies on Human Nutrition by Mass Spectrometric and Nuclear Magnetic Resonance Isotope Ratio Determination. Fresenius Z Anal Chem 324:760–766. doi:10.1007/BF00468387
15. Beavis RC (1993) Chemical Mass of Carbon in Proteins. Anal Chem 65:496–497. doi:10.1021/ac00052a030
16. Carle R (1991) Isotopen-Massenspektrometrie: Grundlagen und Anwendungsmöglichkeiten. Pharm Unserer Zeit 20:75–82. doi:10.1002/pauz.19910200208
17. Ghosh P, Brand WA (2003) Stable Isotope Ratio Mass Spectrometry in Global Climate Change Research. Int J Mass Spectrom 228:1–33. doi:10.1016/S1387-3806(03)00289-6
18. Förstel H (2007) The Natural Fingerprint of Stable Isotopes-Use of IRMS to Test Food Authenticity. Anal Bioanal Chem 388:541–544. doi:10.1007/s00216-007-1241-z
19. Zazzo A, Monahan FJ, Moloney AP, Green S, Schmidt O (2011) Sulphur Isotopes in Animal Hair Track Distance to Sea. Rapid Commun Mass Spectrom 25:2371–2378. doi:10.1002/rcm.5131
20. Busch KL (1997) Isotopes and Mass Spectrometry. Spectroscopy 12:22–26
21. Beynon JH (1960) The compilation of a table of mass and abundance values. In: Mass Spectrometry and Its Applications to Organic Chemistry. Elsevier, Amsterdam
22. Margrave JL, Polansky RB (1962) Relative Abundance Calculations for Isotopic Molecular Species. J Chem Educ 39:335–337. doi:10.1021/ed039p335
23. Yergey JA (1983) A General Approach to Calculating Isotopic Distributions for Mass Spectrometry. Int J Mass Spectrom Ion Phys 52:337–349. doi:10.1016/0020-7381(83)85053-0
24. Hsu CS (1984) Diophantine Approach to Isotopic Abundance Calculations. Anal Chem 56:1356–1361. doi:10.1021/ac00272a035
25. Kubinyi H (1991) Calculation of Isotope Distributions in Mass Spectrometry. A Trivial Solution for a Non-Trivial Problem. Anal Chim Acta 247:107–119. doi:10.1016/S0003-2670(00)83059-7
26. https://sites.google.com/site/isoproms/home
27. http://www.sisweb.com/mstools/isotope.htm
28. Frauenkron M, Berkessel A, Gross JH (1997) Analysis of Ruthenium Carbonyl-Porphyrin Complexes: a Comparison of Matrix-Assisted Laser Desorption/Ionization Time-of-Flight, Fast-Atom Bombardment and Field Desorption Mass Spectrometry. Eur Mass Spectrom 3:427–438. doi:10.1255/ejms.177
29. Giesa S, Gross JH, Hull WE, Lebedkin S, Gromov A, Krätschmer W, Gleiter R (1999) $C_{120}OS$: the First Sulfur-Containing Dimeric [60]Fullerene Derivative. Chem Commun:465–466. doi:10.1039/a809831j
30. Luffer DR, Schram KH (1990) Electron Ionization Mass Spectrometry of Synthetic C_{60}. Rapid Commun Mass Spectrom 4:552–556. doi:10.1002/rcm.1290041218
31. Srivastava SK, Saunders W (1993) Ionization of C_{60} (Buckminsterfullerene) by Electron Impact. Rapid Commun Mass Spectrom 7:610–613. doi:10.1002/rcm.1290070711
32. Scheier P, Dünser B, Märk TD (1995) Production and Stability of Multiply-Charged C_{60}. Electrochem Soc Proc 95:1378–1394

33. Thomas AF (1971) Deuterium Labeling in Organic Chemistry. Appleton-Century-Crofts, New York
34. Kaltashov IA, Eyles SJ (2005) Mass Spectrometry in Biophysics: Conformation and Dynamics of Biomolecules. Wiley, Hoboken
35. Murray KK, Boyd RK, Eberlin MN, Langley GJ, Li L, Naito Y (2013) Definitions of Terms Relating to Mass Spectrometry (IUPAC Recommendations 2013). Pure Appl Chem 85:1515–1609. doi:10.1351/PAC-REC-06-04-06
36. Balogh MP (2004) Debating Resolution and Mass Accuracy in Mass Spectrometry. Spectroscopy 19:34–38,40
37. Bristow AWT (2006) Accurate Mass Measurement for the Determination of Elemental Formula – A Tutorial. Mass Spectrom Rev 25:99–111. doi:10.1002/mas.20058
38. Leslie AD, Volmer DA (2007) Dealing With the Masses: A Tutorial on Accurate Masses, Mass Uncertainties, and Mass Defects. Spectroscopy 22:32,34–32,39
39. Busch KL (2000) The Resurgence of Exact Mass Measurement With FTMS. Spectroscopy 15:22–27
40. Beynon JH (1954) Qualitative Analysis of Organic Compounds by Mass Spectrometry. Nature 174:735–737. doi:10.1038/174735a0
41. Pomerantz SC, McCloskey JA (1987) Fractional Mass Values of Large Molecules. Org Mass Spectrom 22:251–253. doi:10.1002/oms.1210220505
42. Boyd RK, Basic C, Bethem RA (2008) Trace Quantitative Analysis by Mass Spectrometry. Wiley, Chichester
43. Kilburn KD, Lewis PH, Underwood JG, Evans S, Holmes J, Dean M (1979) Quality of Mass and Intensity Measurements from a High Performance Mass Spectrometer. Anal Chem 51:1420–1425. doi:10.1021/ac50045a017
44. Sack TM, Lapp RL, Gross ML, Kimble BJ (1984) A Method for the Statistical Evaluation of Accurate Mass Measurement Quality. Int J Mass Spectrom Ion Proc 61:191–213. doi:10.1016/0168-1176(84)85129-0
45. Kim S, Rodgers RP, Marshall AG (2006) Truly "Exact" Mass: Elemental Composition Can Be Determined Uniquely from Molecular Mass Measurement at Approximately 0.1 MDa Accuracy for Molecules Up to Approximately 500 Da. Int J Mass Spectrom 251:260–265. doi:10.1016/j.ijms.2006.02.001
46. Zubarev RA, Demirev PA, Håkansson P, Sundqvist BUR (1995) Approaches and Limits for Accurate Mass Characterization of Large Biomolecules. Anal Chem 67:3793–3798. doi:10.1021/ac00116a028
47. Zubarev RA, Håkansson P, Sundqvist B (1996) Accuracy Requirements for Peptide Characterization by Monoisotopic Molecular Mass Measurements. Anal Chem 68:4060–4063. doi:10.1021/ac9604651
48. Clauser KR, Baker P, Burlingame A (1999) Role of Accurate Mass Measurement (±10 ppm) in Protein Identification Strategies Employing MS or MS/MS and Database Searching. Anal Chem 71:2871–2882. doi:10.1021/ac9810516
49. Spengler B (2004) De Novo Sequencing, Peptide Composition Analysis, and Composition-Based Sequencing: A New Strategy Employing Accurate Mass Determination by Fourier Transform Ion Cyclotron Resonance Mass Spectrometry. J Am Soc Mass Spectrom 15:703–714. doi:10.1016/j.jasms.2004.01.007
50. Roussis SG, Proulx R (2003) Reduction of Chemical Formulas from the Isotopic Peak Distributions of High-Resolution Mass Spectra. Anal Chem 75:1470–1482. doi:10.1021/ac020516w
51. Stoll N, Schmidt E, Thurow K (2006) Isotope Pattern Evaluation for the Reduction of Elemental Compositions Assigned to High-Resolution Mass Spectral Data from Electrospray Ionization Fourier Transform Ion Cyclotron Resonance Mass Spectrometry. J Am Soc Mass Spectrom 17:1692–1699. doi:10.1016/j.jasms.2006.07.022
52. Marshall AG, Hendrickson CL, Shi SDH (2002) Scaling MS Plateaus with High-Resolution FT-ICR-MS. Anal Chem 74:252A–259A. doi:10.1021/ac022010j

53. Sim PG, Boyd RK (1991) Calibration and Mass Measurement in Negative-Ion Fast-Atom Bombardment Mass Spectrometry. Rapid Commun Mass Spectrom 5:538–542. doi:10.1002/rcm.1290051111
54. Anacleto JF, Pleasance S, Boyd RK (1992) Calibration of Ion Spray Mass Spectra Using Cluster Ions. Org Mass Spectrom 27:660–666. doi:10.1002/oms.1210270603
55. Hop CECA (1996) Generation of High Molecular Weight Cluster Ions by Electrospray Ionization; Implications for Mass Calibration. J Mass Spectrom 31:1314–1316. doi:10.1002/(SICI)1096-9888(199611)31:11<1314::AID-JMS429>3.0.CO;2-N
56. Moini M, Jones BL, Rogers RM, Jiang L (1998) Sodium Trifluoroacetate as a Tune/Calibration Compound for Positive- and Negative-Ion Electrospray Ionization Mass Spectrometry in the Mass Range of 100–4000 Da. J Am Soc Mass Spectrom 9:977–980. doi:10.1016/S1044-0305(98)00079-8
57. Lou X, van Dongen JLJ, Meijer EW (2010) Generation of CsI Cluster Ions for Mass Calibration in Matrix-Assisted Laser Desorption/Ionization Mass Spectrometry. J Am Soc Mass Spectrom 21:1223–1226. doi:10.1016/j.jasms.2010.02.029
58. Gross JH (2014) High-Mass Cluster Ions of Ionic Liquids in Positive-Ion and Negative-Ion DART-MS and Their Application for Wide Range Mass Calibrations. Anal Bioanal Chem 406:2853–2862. doi:10.1007/s00216-014-7720-0
59. Busch KL (2004) Masses in Mass Spectrometry: Balancing the Analytical Scales. Spectroscopy 19:32–34
60. Busch KL (2005) Masses in Mass Spectrometry: Perfluors and More. Part II. Spectroscopy 20:76–81
61. Gross ML (1994) Accurate Masses for Structure Confirmation. J Am Soc Mass Spectrom 5:57. doi:10.1016/1044-0305(94)85036-4
62. Bristow AWT, Webb KS (2003) Intercomparison Study on Accurate Mass Measurement of Small Molecules in Mass Spectrometry. J Am Soc Mass Spectrom 14:1086–1098. doi:10.1016/S1044-0305(03)00403-3
63. Pluskal T, Uehara T, Yanagida M (2012) Highly Accurate Chemical Formula Prediction Tool Utilizing High-Resolution Mass Spectra, MS/MS Fragmentation, Heuristic Rules, and Isotope Pattern Matching. Anal Chem 84:4396–4403. doi:10.1021/ac3000418
64. Thurman EM, Ferrer I (2010) The Isotopic Mass Defect: a Tool for Limiting Molecular Formulas by Accurate Mass. Anal Bioanal Chem 397:2807–2816. doi:10.1007/s00216-010-3562-6
65. Gross JH (2013) Polydimethylsiloxane-Based Wide Range Mass Calibration for Direct Analysis in Real Time Mass Spectrometry. Anal Bioanal Chem 405:8663–8668. doi:10.1007/s00216-013-7287-1
66. Gross JH (2015) Polydimethylsiloxane Extraction from Silicone Rubber into Baked Goods Detected by Direct Analysis in Real Time Mass Spectrometry. Eur J Mass Spectrom 21:313–319. doi:10.1255/ejms.1333
67. Yergey J, Heller D, Hansen G, Cotter RJ, Fenselau C (1983) Isotopic Distributions in Mass Spectra of Large Molecules. Anal Chem 55:353–356. doi:10.1021/ac00253a037
68. Werlen RC (1994) Effect of Resolution on the Shape of Mass Spectra of Proteins: Some Theoretical Considerations. Rapid Commun Mass Spectrom 8:976–980. doi:10.1002/rcm.1290081214
69. Solouki T, Emmet MR, Guan S, Marshall AG (1997) Detection, Number, and Sequence Location of Sulfur-Containing Amino Acids and Disulfide Bridges in Peptides by Ultrahigh-Resolution MALDI-FTICR Mass Spectrometry. Anal Chem 69:1163–1168. doi:10.1021/ac960885q
70. Nikolaev EN, Jertz R, Grigoryev A, Baykut G (2012) Fine Structure in Isotopic Peak Distributions Measured Using a Dynamically Harmonized Fourier Transform Ion Cyclotron Resonance Cell at 7 T. Anal Chem 84:2275–2283. doi:10.1021/ac202804f
71. Popov IA, Nagornov K, Vladimirov GN, Kostyukevich YI, Nikolaev EN (2014) Twelve Million Resolving Power on 4.7 T Fourier Transform Ion Cyclotron Resonance Instrument

With Dynamically Harmonized Cell-Observation of Fine Structure in Peptide Mass Spectra. J Am Soc Mass Spectrom 25:790–799. doi:10.1007/s13361-014-0846-7
72. Matsuo T, Sakurai T, Ito H, Wada Y (1991) High Masses. Int J Mass Spectrom Ion Proc 118 (119):635–659. doi:10.1016/0168-1176(92)85079-F
73. Grayson SM, Myers BK, Bengtsson J, Malkoch M (2014) Advantages of Monodisperse and Chemically Robust "SpheriCal" Polyester Dendrimers as a "Universal" MS Calibrant. J Am Soc Mass Spectrom 25:303–309. doi:10.1007/s13361-013-0777-8
74. Gross JH (2016) Improved Procedure for Dendrimer-Based Mass Calibration in Matrix-Assisted Laser Desorption/Ionization-Time-of-Flight–Mass Spectrometry. Anal Bioanal Chem 408:5945–5951. doi:10.1007/s00216-016-9714-6
75. Lehmann WD, Bohne A, von der Lieth CW (2000) The Information Encrypted in Accurate Peptide Masses – Improved Protein Identification and Assistance in Glycopeptide Identification and Characterization. J Mass Spectrom 35:1335–1341. doi:10.1002/1096-9888(200011)35:11<1335::AID-JMS70>3.0.CO;2-0
76. Kendrick E (1963) Mass Scale Based on $CH_2 = 14.0000$ for High-Resolution Mass Spectrometry of Organic Compounds. Anal Chem 35:2146–2154. doi:10.1021/ac60206a048
77. Hughey CA, Hendrickson CL, Rodgers RP, Marshall AG, Qian K (2001) Kendrick Mass Defect Spectrum: A Compact Visual Analysis for Ultrahigh-Resolution Broadband Mass Spectra. Anal Chem 73:4676–4681. doi:10.1021/ac010560w
78. Jobst KJ, Shen L, Reiner EJ, Taguchi VY, Helm PA, McCrindle R, Backus S (2013) The Use of Mass Defect Plots for the Identification of (Novel) Halogenated Contaminants in the Environment. Anal Bioanal Chem 405:3289–3297. doi:10.1007/s00216-013-6735-2
79. Myers AL, Jobst KJ, Mabury SA, Reiner EJ (2014) Using Mass Defect Plots As a Discovery Tool to Identify Novel Fluoropolymer Thermal Decomposition Products. J Mass Spectrom 49:291–296. doi:10.1002/jms.3340
80. Ibanez C, Simo C, Garcia-Canas V, Acunha T, Cifuentes A (2015) The Role of Direct High-Resolution Mass Spectrometry in Foodomics. Anal Bioanal Chem 407:6275–6287. doi:10.1007/s00216-015-8812-1
81. Fouquet T, Sato H (2016) Convenient Visualization of High-Resolution Tandem Mass Spectra of Synthetic Polymer Ions Using Kendrick Mass Defect Analysis – The Case of Polysiloxanes. Rapid Commun Mass Spectrom 30:1361–1364. doi:10.1002/rcm.7560
82. Hughey CA, Hendrickson CL, Rodgers RP, Marshall AG (2001) Elemental Composition Analysis of Processed and Unprocessed Diesel Fuel by Electrospray Ionization Fourier Transform Ion Cyclotron Resonance Mass Spectrometry. Energy & Fuels 15:1186–1193. doi:10.1021/ef010028b
83. van Krevelen DW (1950) Graphical-Statistical Method for the Study of Structure and Reaction Processes of Coal. Fuel 29:269–284
84. Wu Z, Rodgers RP, Marshall AG (2004) Two- and Three-Dimensional Van Krevelen Diagrams: A Graphical Analysis Complementary to the Kendrick Mass Plot for Sorting Elemental Compositions of Complex Organic Mixtures Based on Ultrahigh-Resolution Broadband Fourier Transform Ion Cyclotron Resonance Mass Measurements. Anal Chem 76:2511–2516. doi:10.1021/ac0355449
85. Kim S, Kramer RW, Hatcher PG (2003) Graphical Method for Analysis of Ultrahigh-Resolution Broadband Mass Spectra of Natural Organic Matter, the Van Krevelen Diagram. Anal Chem 75:5336–5344. doi:10.1021/ac034415p
86. Hertkorn N, Benner R, Frommberger M, Schmitt-Kopplin P, Witt M, Kaiser K, Kettrup A, Hedges JI (2006) Characterization of a Major Refractory Component of Marine Dissolved Organic Matter. Geochim Cosmochim Acta 70:2990–3010. doi:10.1016/j.gca.2006.03.021
87. Dittmar T, Koch BP (2006) Thermogenic Organic Matter Dissolved in the Abyssal Ocean. Marine Chem 102:208–217. doi:10.1016/j.marchem.2006.04.003
88. Koch BP, Dittmar T (2005) From Mass to Structure: an Aromaticity Index for High-Resolution Mass Data of Natural Organic Matter. Rapid Commun Mass Spectrom 20:926–932. doi:10.1002/rcm.2386